Deep Learning in CT Artifact Correction

Marc Kachelrieß

German Cancer Research Center (DKFZ)
Heidelberg, Germany
www.dkfz.de/ct

dkfz. DEUTSCHES KREBSFORSCHUNGSZENTRUM IN DER HELMHOLTZ-GEMEINSCHAFT

Content

- Metal artifact reduction (MAR)
- Ring artifact reduction (RAR)
- Detruncation
- Scatter estimation
- Motion compensation
- Sparse view artifacts
- Limited angle artifacts

Deep MAR Examples

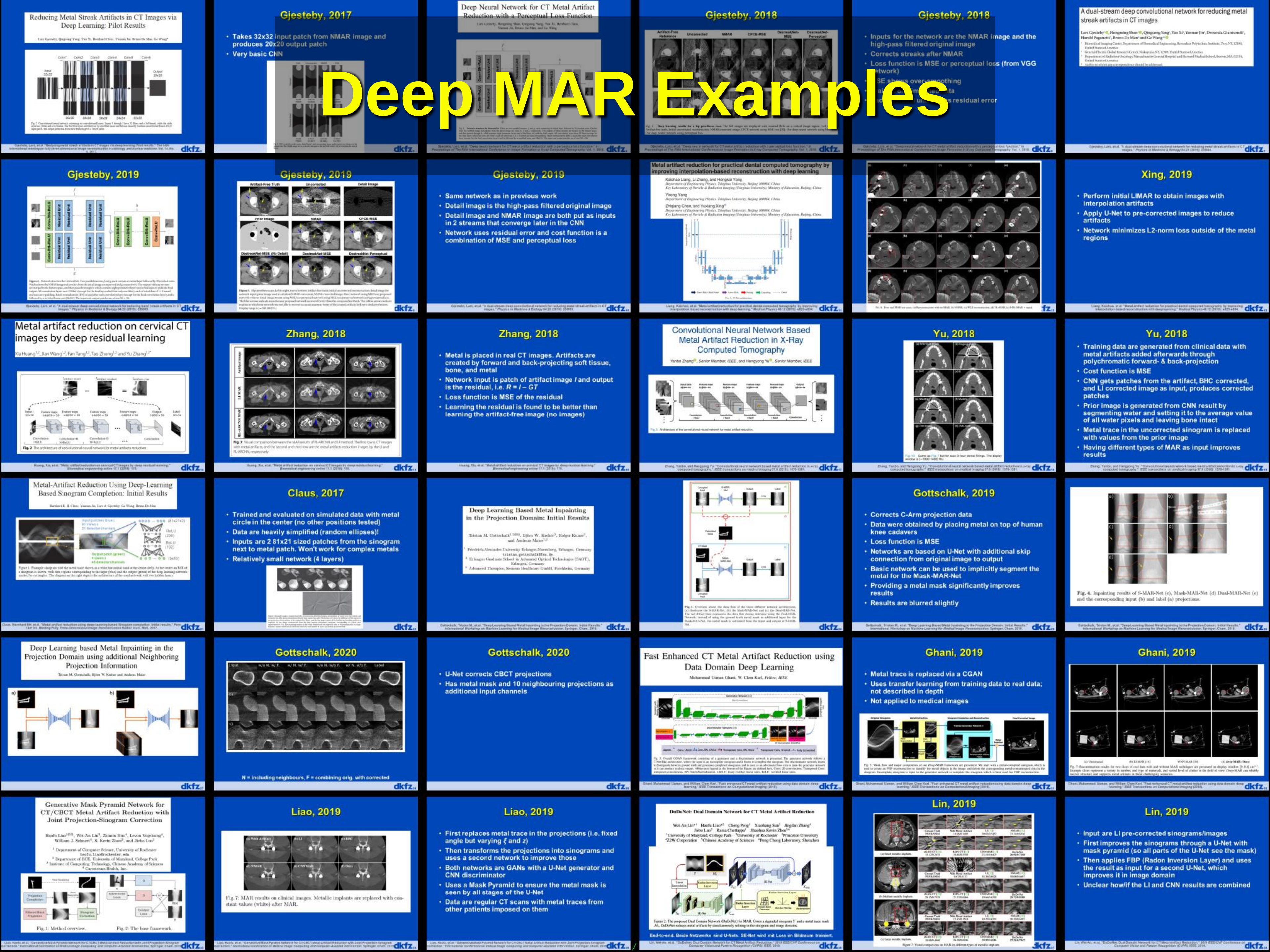

Metal artifact reduction for practical dental computed tomography by improving interpolation-based reconstruction with deep learning

Kaichao Liang, Li Zhang, and Hongkai Yang
Department of Engineering Physics, Tsinghua University, Beijing 100084, China
Key Laboratory of Particle & Radiation Imaging (Tsinghua University), Ministry of Education, Beijing, China

Yirong Yang
Department of Engineering Physics, Tsinghua University, Beijing 100084, China

Zhiqiang Chen, and Yuxiang Xing[a)]
Department of Engineering Physics, Tsinghua University, Beijing 100084, China
Key Laboratory of Particle & Radiation Imaging (Tsinghua University), Ministry of Education, Beijing, China

LI-MAR image in

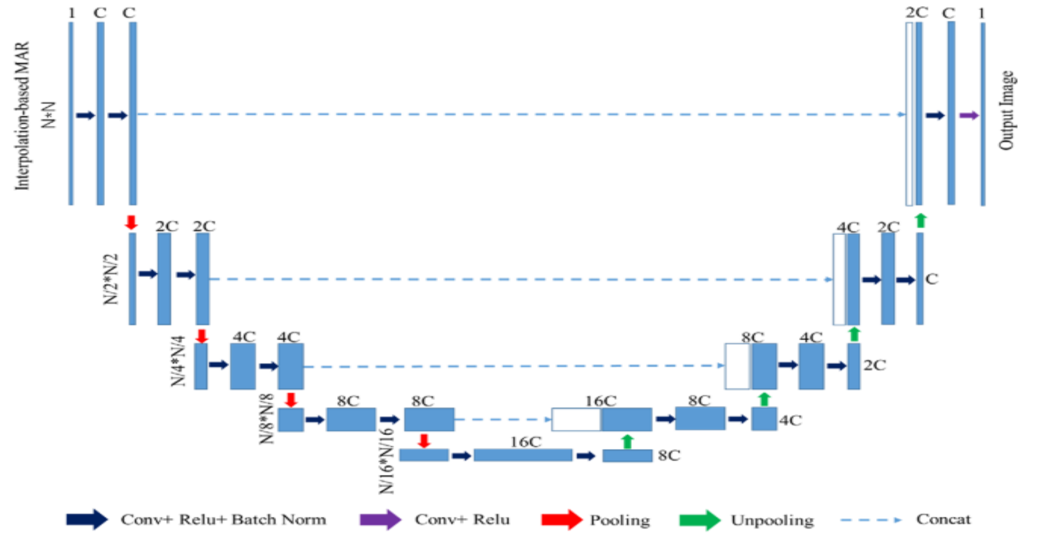

FIG. 3. U-Net architecture.

nicer image out

Liang, Kaichao, et al. "Metal artifact reduction for practical dental computed tomography by improving interpolation-based reconstruction with deep learning." *Medical Physics* 46.12 (2019): e823-e834.

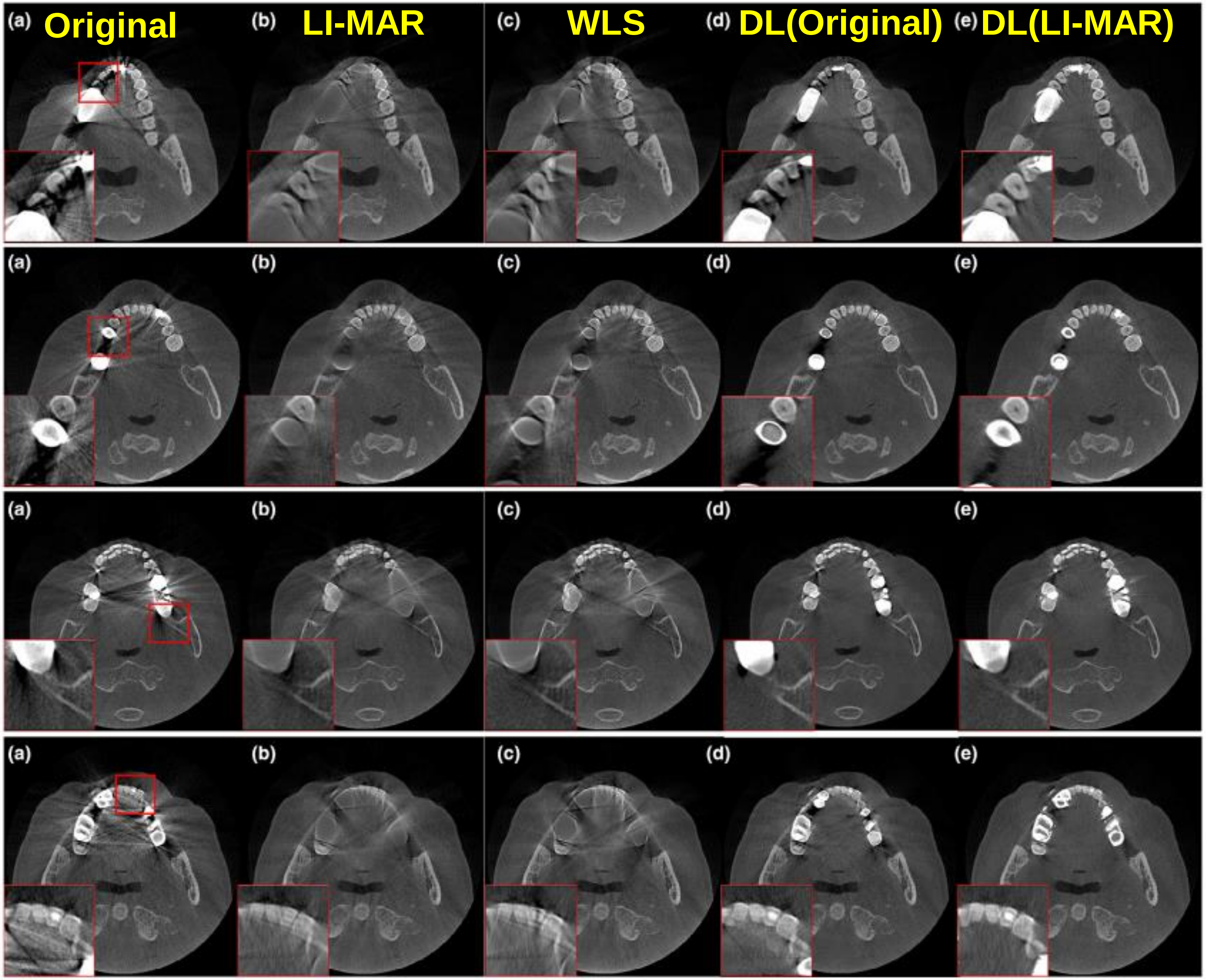

FIG. 8. Four real MAR test cases. (a) Reconstructions with no MAR, (b) I-MAR, (c) WLS reconstruction, (d) DL-MAR, (e) I-DL-MAR + metal.

MAR Example

- Deep CNN-driven patch-based combination of the advantages of several MAR methods trained on simulated artifacts

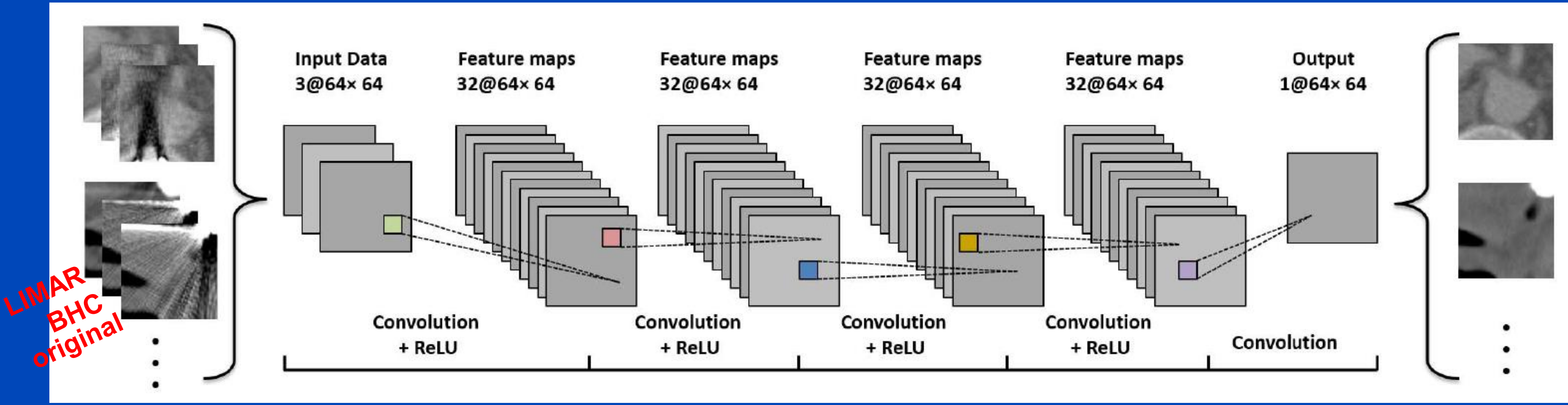

- followed by segmentation into tissue classes
- followed by forward projection of the CNN prior and replacement of metal areas of the original sinogram
- followed by reconstruction

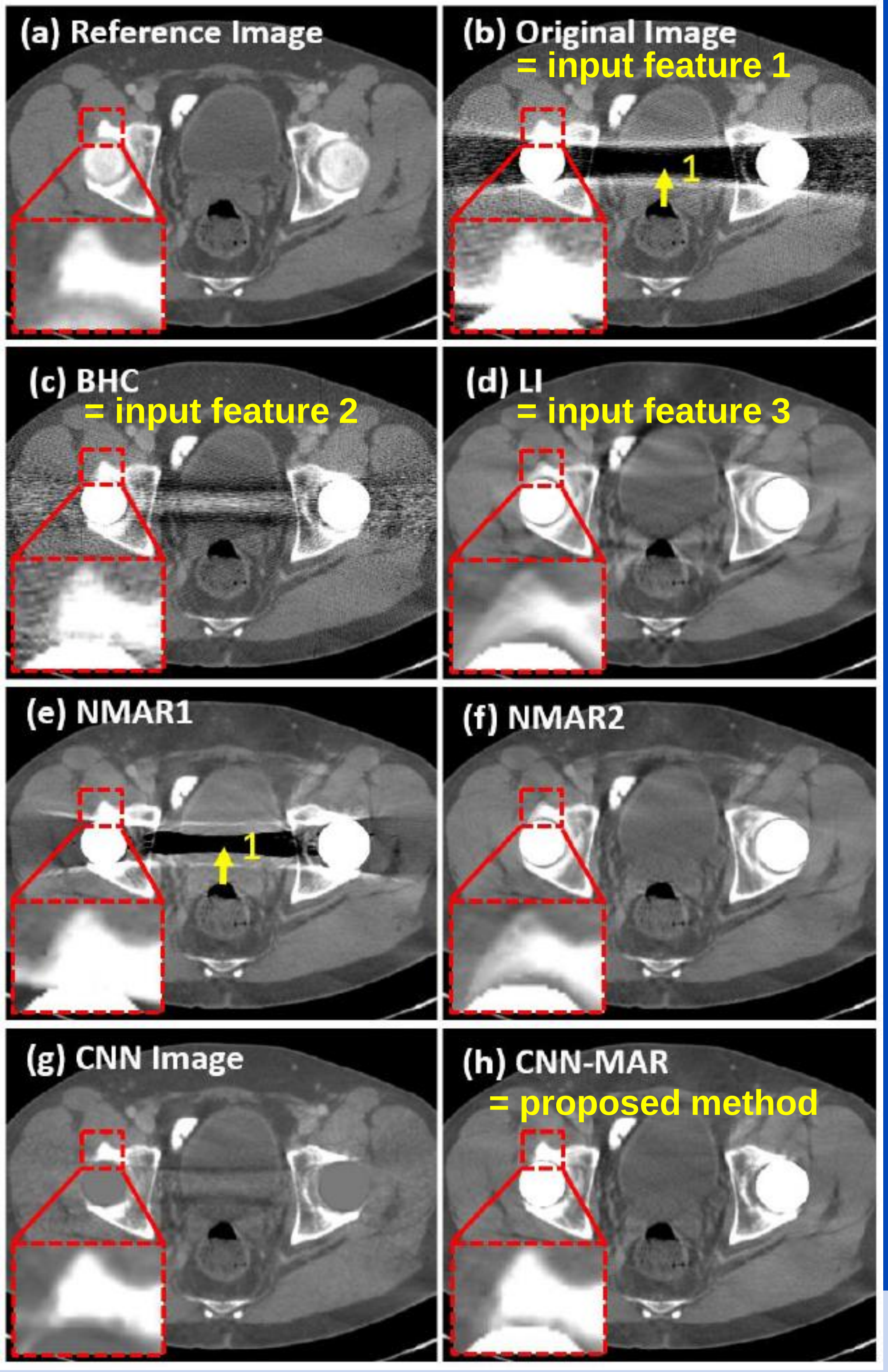
(a) Reference Image
(b) Original Image
= input feature 1
1
(c) BHC
= input feature 2
(d) LI
= input feature 3
(e) NMAR1
1
(f) NMAR2
(g) CNN Image
(h) CNN-MAR
= proposed method

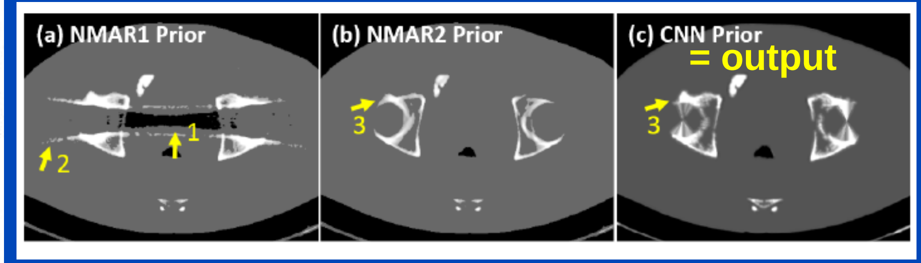
(a) NMAR1 Prior
1
2
(b) NMAR2 Prior
3
(c) CNN Prior
= output
3

dkfz.

MAR without Machine Learning is a Good Alternative: Frequency Split Normalized MAR[1,2]

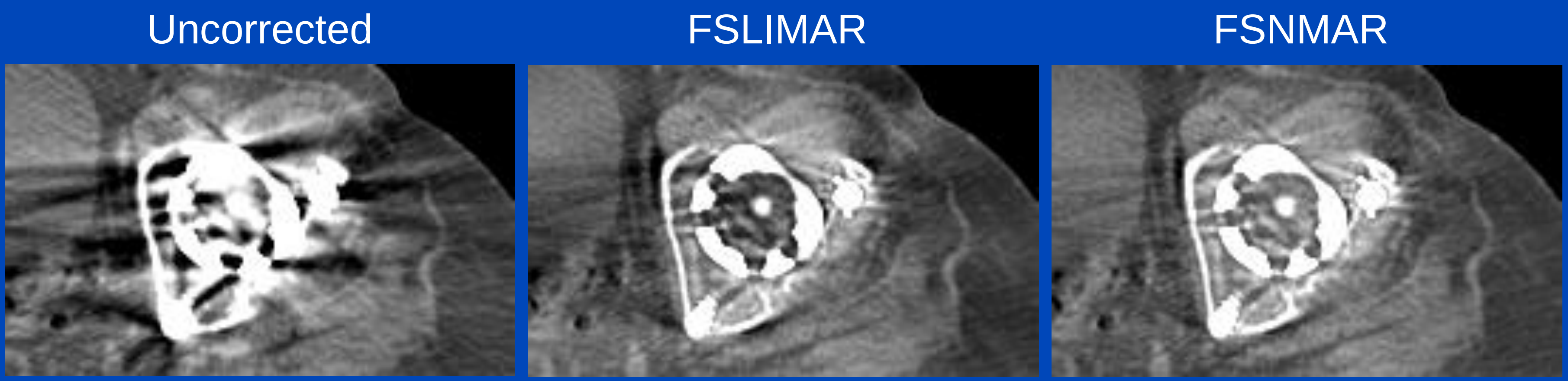

Patient with bilateral hip prosthesis, Somatom Definition Flash, (C = 40 HU, W = 500 HU).

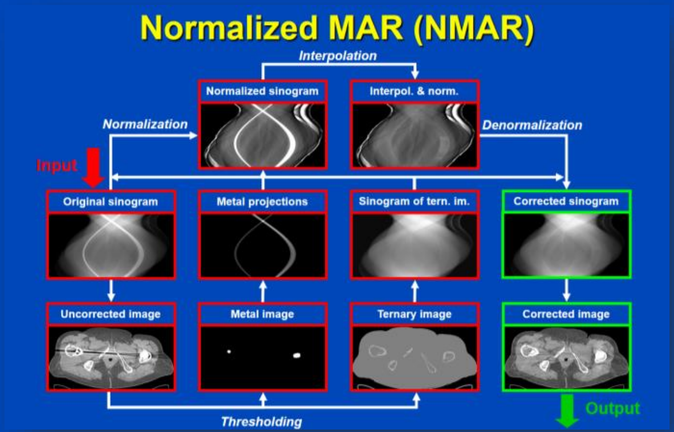

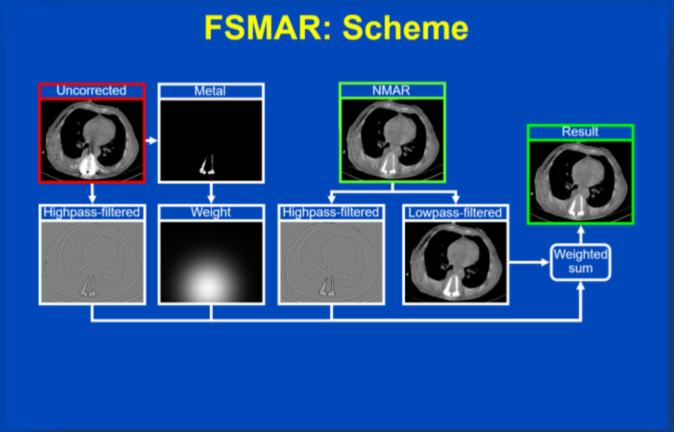

[1]E. Meyer, M. Kachelrieß. Normalized metal artifact reduction (NMAR) in computed tomography. Med. Phys. 37(10):5482-5493, Oct. 2010.
[2]E. Meyer, M. Kachelrieß. Frequency split metal artifact reduction (FSMAR) in CT. Med. Phys. 39(4):1904-1916, April 2012.

Summary on Deep MAR

- **Most common uses for networks:**
  - Improve image quality in image domain after MAR
  - Use network for the sinogram inpainting
  - Produce a prior image, e.g. for NMAR
- **Additional observations:**
  - Training data are often produced by segmenting an artifact-free CT image, adding metal and applying a polychromatic forward projection to different types of tissue separately.
  - As of today, it seems hard to outperform NMAR, or hard to give convincing clinical examples.

Deep Detruncation

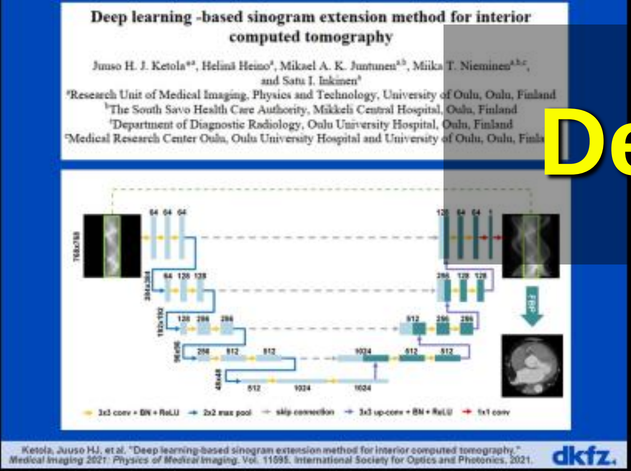

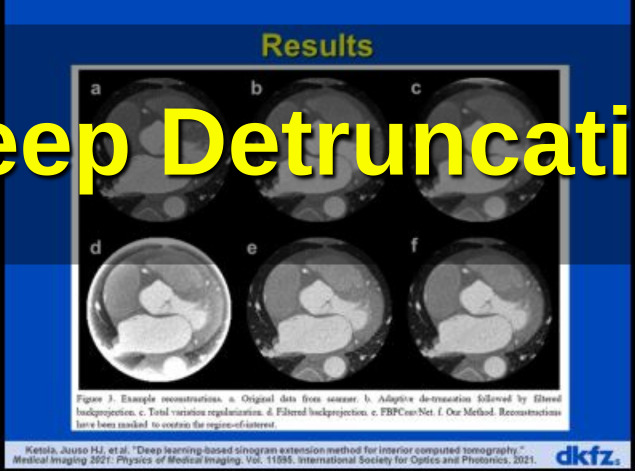

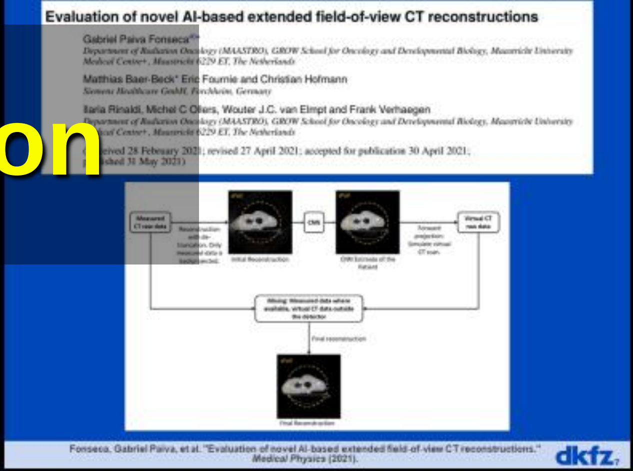

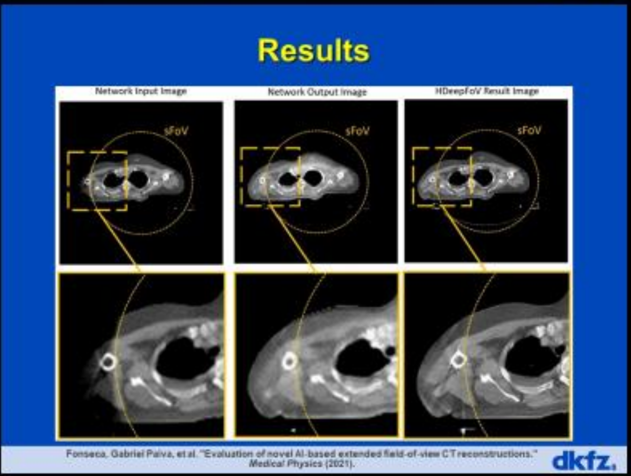

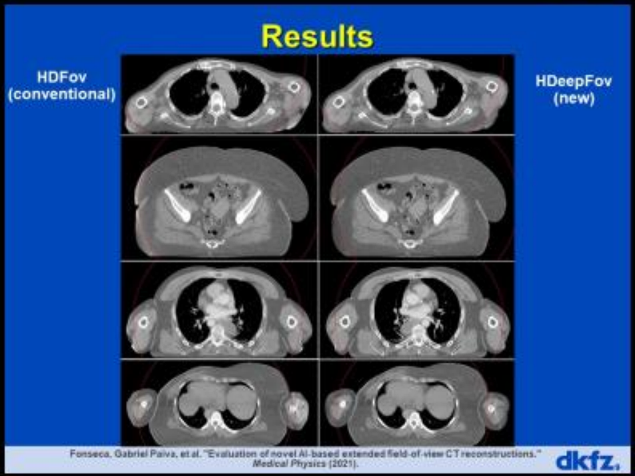

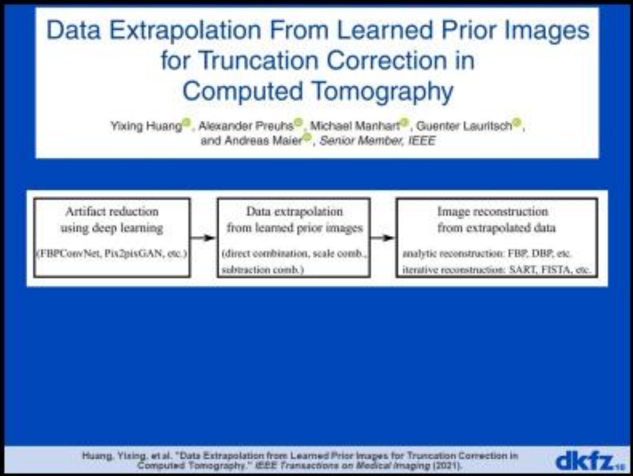

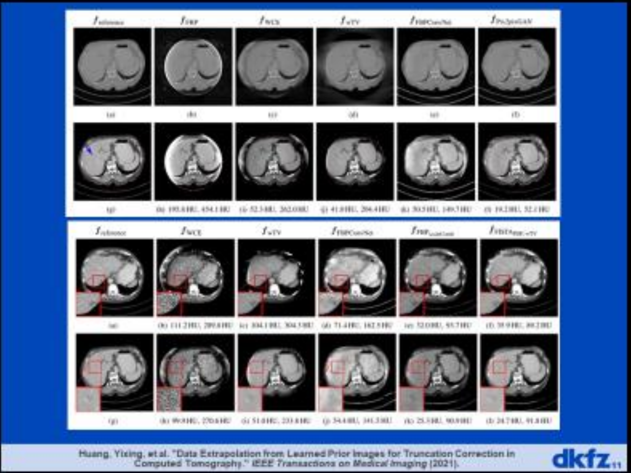

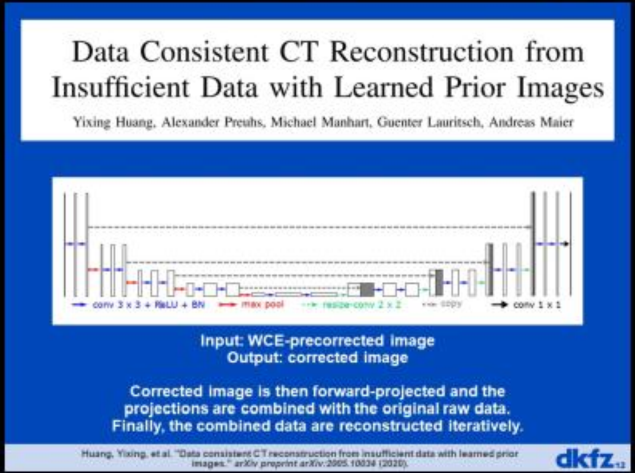

Deep learning -based sinogram extension method for interior computed tomography

Juuso H. J. Ketola*[a], Helinä Heino[a], Mikael A. K. Juntunen[a,b], Miika T. Nieminen[a,b,c], and Satu I. Inkinen[a]
[a]Research Unit of Medical Imaging, Physics and Technology, University of Oulu, Oulu, Finland
[b]The South Savo Health Care Authority, Mikkeli Central Hospital, Oulu, Finland
[c]Department of Diagnostic Radiology, Oulu University Hospital, Oulu, Finland
[c]Medical Research Center Oulu, Oulu University Hospital and University of Oulu, Oulu, Finland

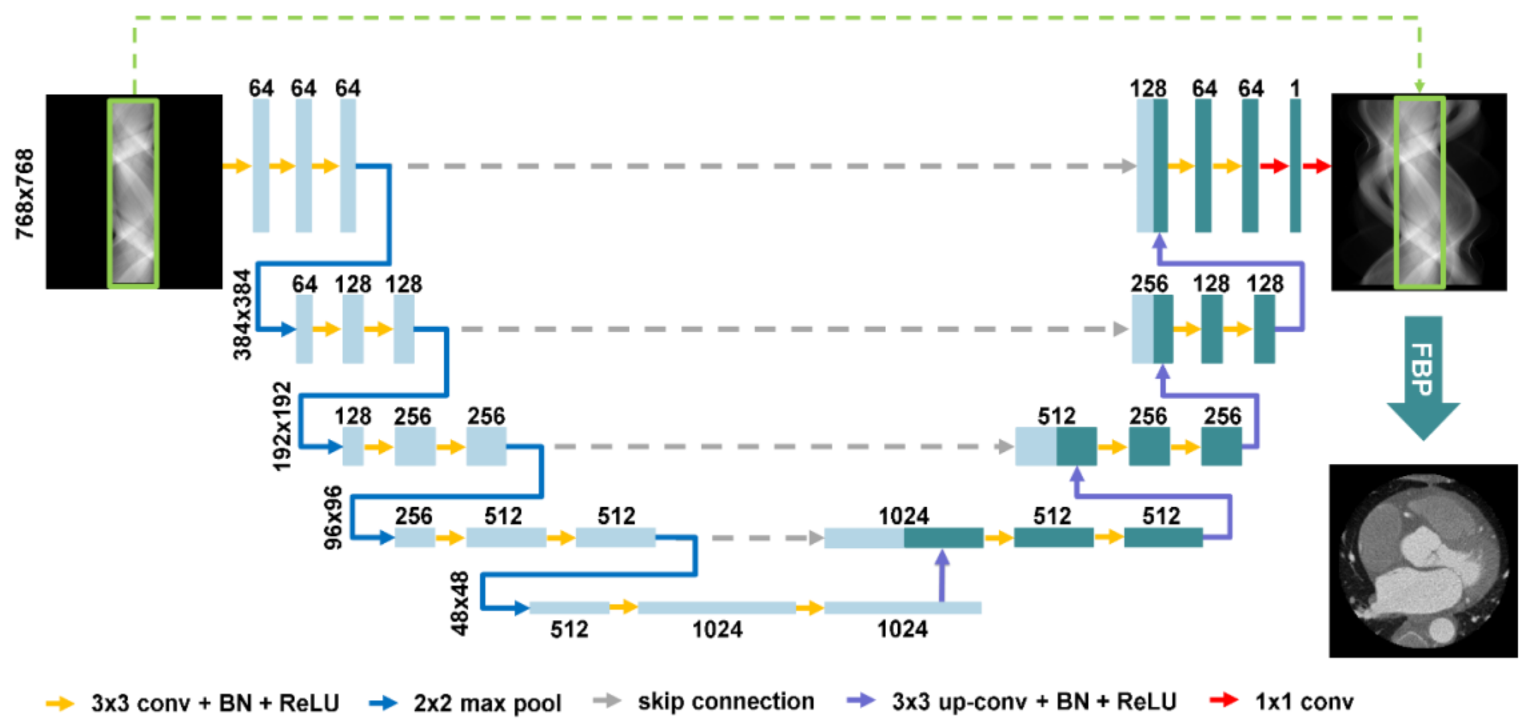

Ketola, Juuso HJ, et al. "Deep learning-based sinogram extension method for interior computed tomography."
Medical Imaging 2021: Physics of Medical Imaging. Vol. 11595. International Society for Optics and Photonics, 2021.

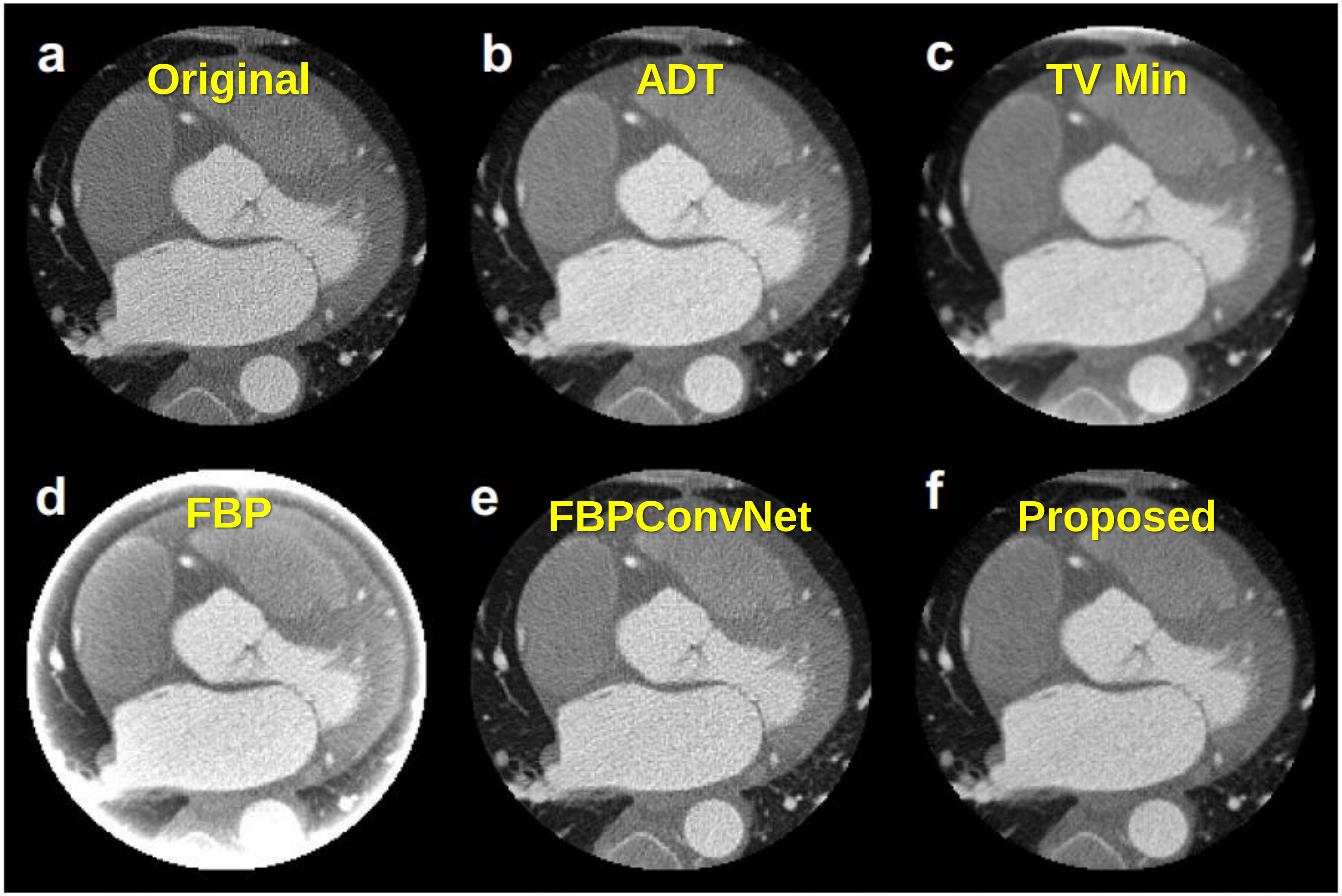

Figure 3. Example reconstructions. a. Original data from scanner. b. Adaptive de-truncation followed by filtered backprojection. c. Total variation regularization. d. Filtered backprojection. e. FBPConvNet. f. Our Method. Reconstructions have been masked to contain the region-of-interest.

Evaluation of novel AI-based extended field-of-view CT reconstructions

Gabriel Paiva Fonseca[a)*]
Department of Radiation Oncology (MAASTRO), GROW School for Oncology and Developmental Biology, Maastricht University Medical Centre+, Maastricht 6229 ET, The Netherlands

Matthias Baer-Beck[*] Eric Fournie and Christian Hofmann
Siemens Healthcare GmbH, Forchheim, Germany

Ilaria Rinaldi, Michel C Ollers, Wouter J.C. van Elmpt and Frank Verhaegen
Department of Radiation Oncology (MAASTRO), GROW School for Oncology and Developmental Biology, Maastricht University Medical Centre+, Maastricht 6229 ET, The Netherlands

(Received 28 February 2021; revised 27 April 2021; accepted for publication 30 April 2021; published 31 May 2021)

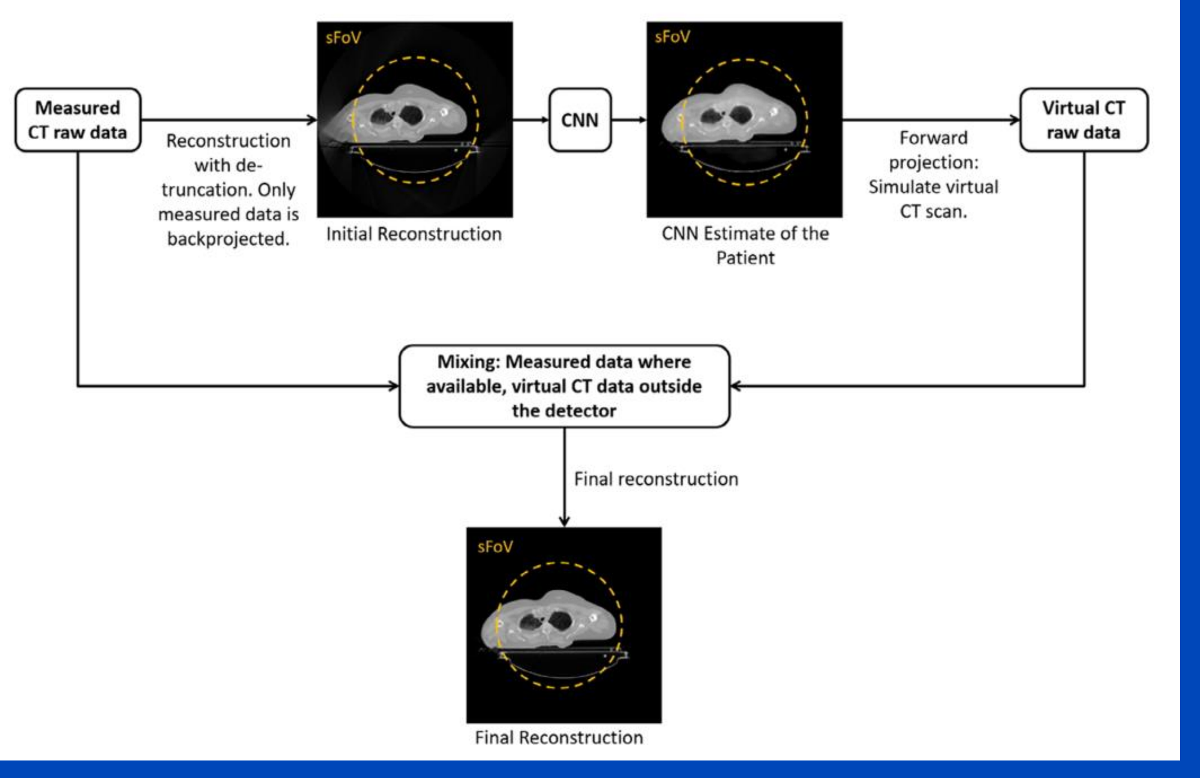

Fonseca, Gabriel Paiva, et al. "Evaluation of novel AI-based extended field-of-view CT reconstructions." *Medical Physics* (2021).

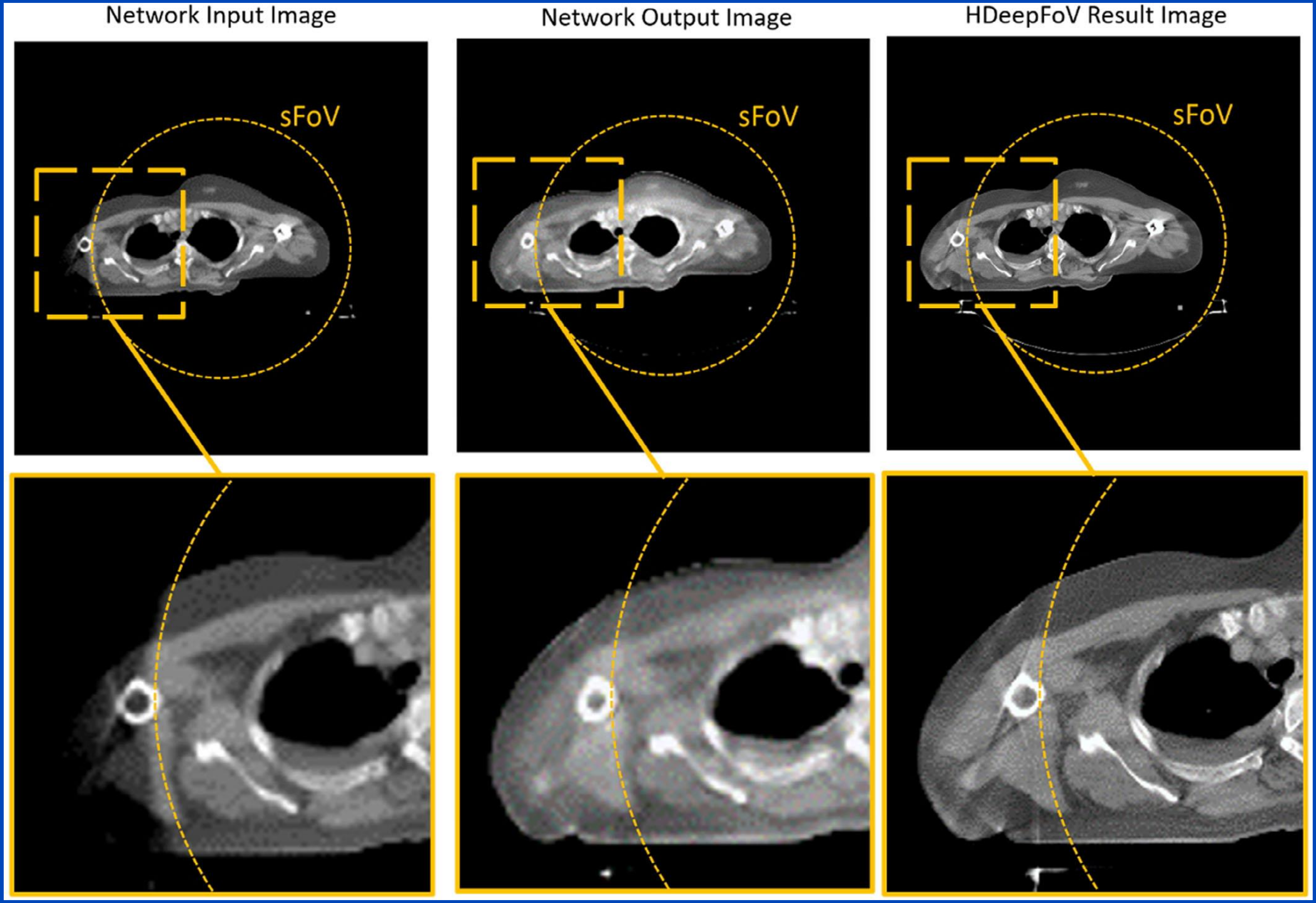

Fonseca, Gabriel Paiva, et al. "Evaluation of novel AI-based extended field-of-view CT reconstructions." *Medical Physics* (2021).

Original

Truncated

ADT corrected

ADT corrected (clipped)

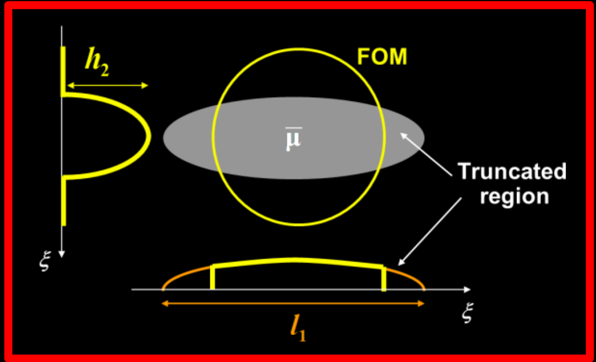

C = 0 HU, W = 1000 HU

K. Sourbelle, M. Kachelrieß, and W.A. Kalender, "Reconstruction from truncated projections in CT using adaptive detruncation," Eur Radiol 15:1008–1014, 2005.

Summary on Deep Detruncation

- No need for machine learning to restore the gray values within the FOM
- Image domain cosmetic detruncation can serve as an intermediate step to detruncate CT data.

Deep Scatter Estimation

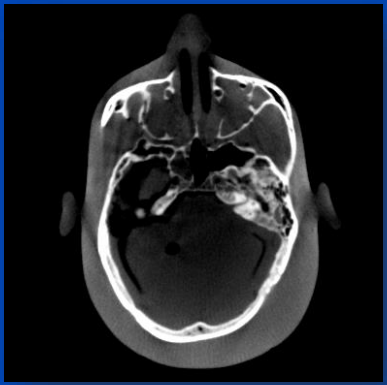

???

In real time?

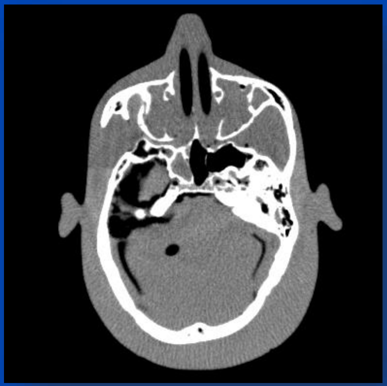

Monte Carlo Scatter Estimation

- Simulation of photon trajectories according to physical interaction probabilities.
- Simulating a large numb… …ories well approximat…

1 hour
per tomographic data set

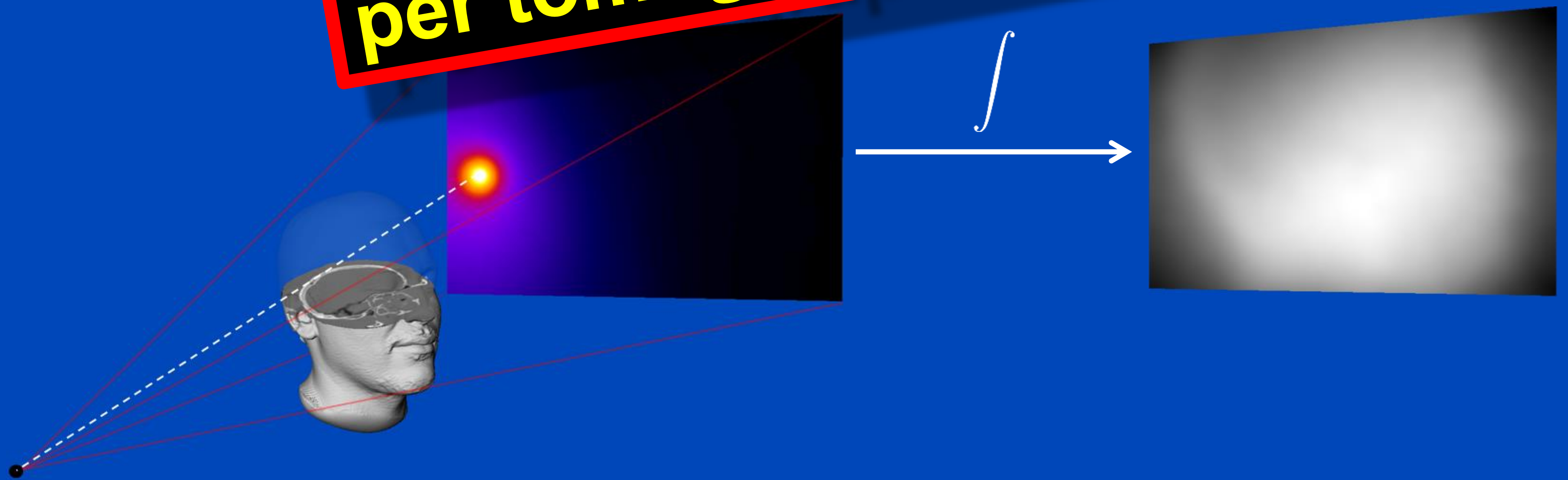

Deep Scatter Estimation

Network architecture & scatter estimation framework

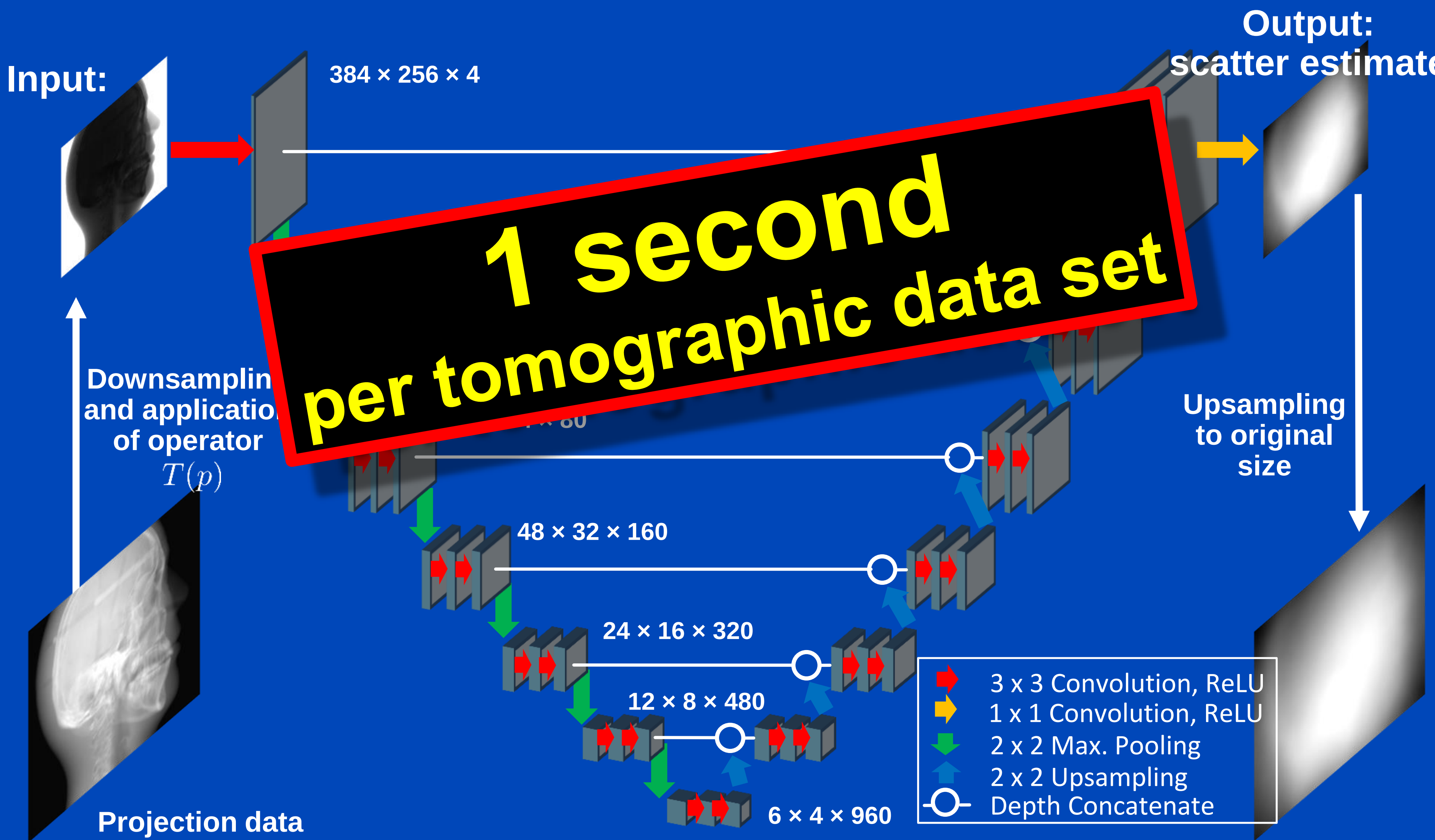

J. Maier, M. Kachelrieß et al. Deep scatter estimation (DSE). SPIE 2017 and Journal of Nondestructive Evaluation 37:57, July 2018.
J. Maier, M. Kachelrieß et al. Robustness of DSE. Med. Phys. 46(1):238-249, January 2019.

Testing of the DSE Network for Measured Data (120 kV)

DKFZ table-top CT

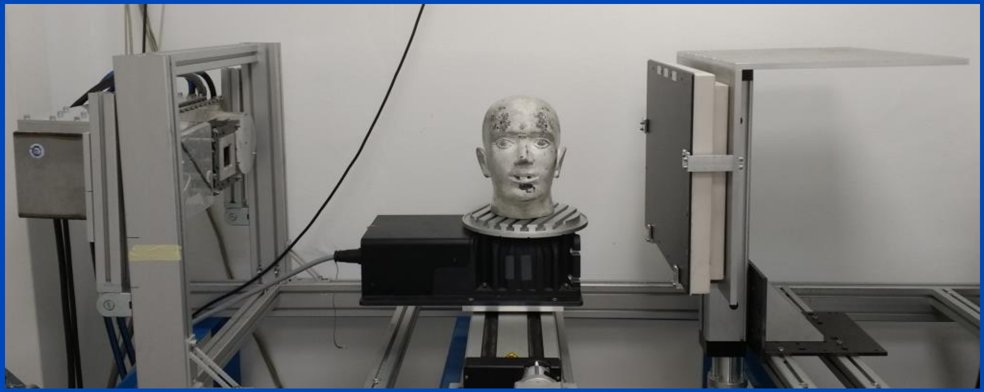

- Measurement of a head phantom at our in-house table-top CT.
- Slit scan measurement serves as ground truth.

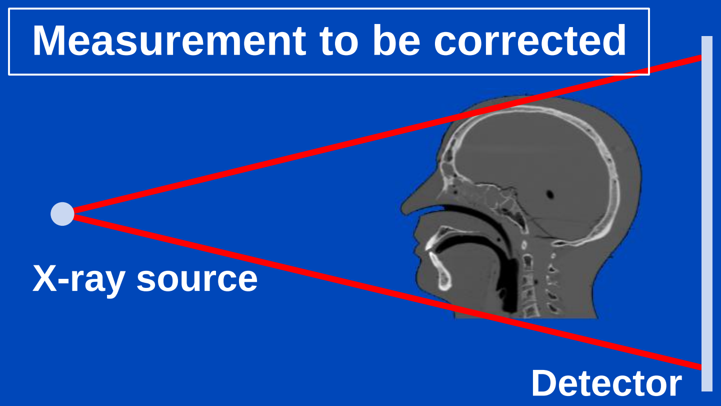

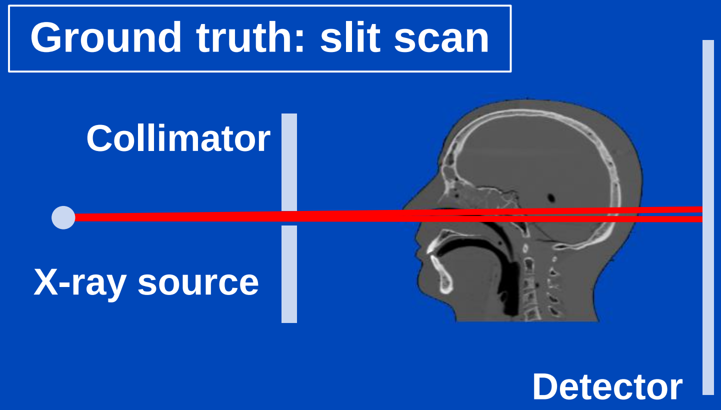

J. Maier, M. Kachelrieß et al. Deep scatter estimation (DSE). SPIE 2017 and Journal of Nondestructive Evaluation 37:57, July 2018.
J. Maier, M. Kachelrieß et al. Robustness of DSE. Med. Phys. 46(1):238-249, January 2019.

Reconstructions of Measured Data

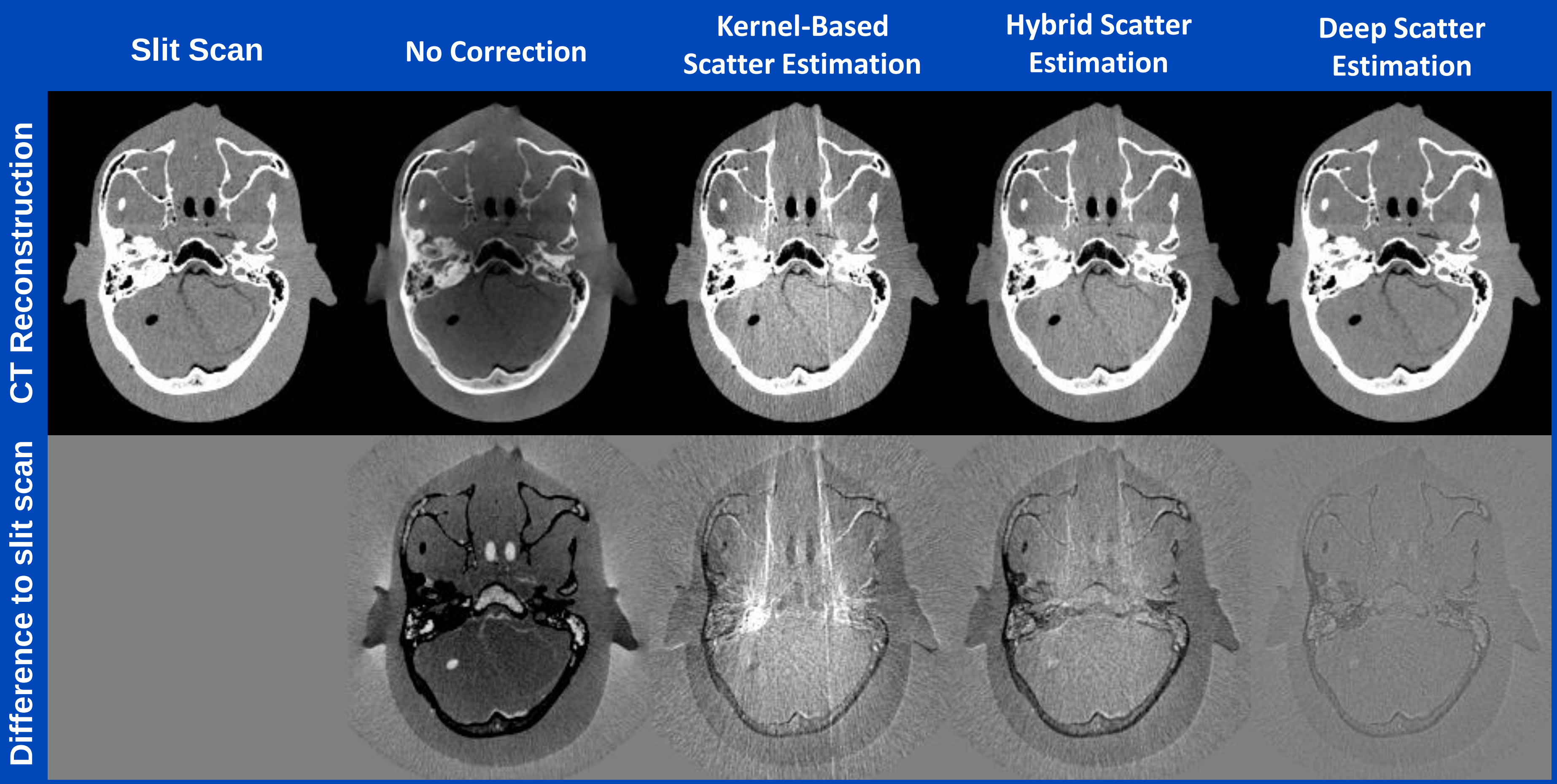

C = 0 HU, W = 1000 HU

J. Maier, M. Kachelrieß et al. Deep scatter estimation (DSE). SPIE 2017 and Journal of Nondestructive Evaluation 37:57, July 2018.
J. Maier, M. Kachelrieß et al. Robustness of DSE. Med. Phys. 46(1):238-249, January 2019.

A simple detruncation was applied to the rawdata before reconstruction. Images were clipped to the FOM before display. C = -200 HU, W = 1000 HU.

Truncated DSE

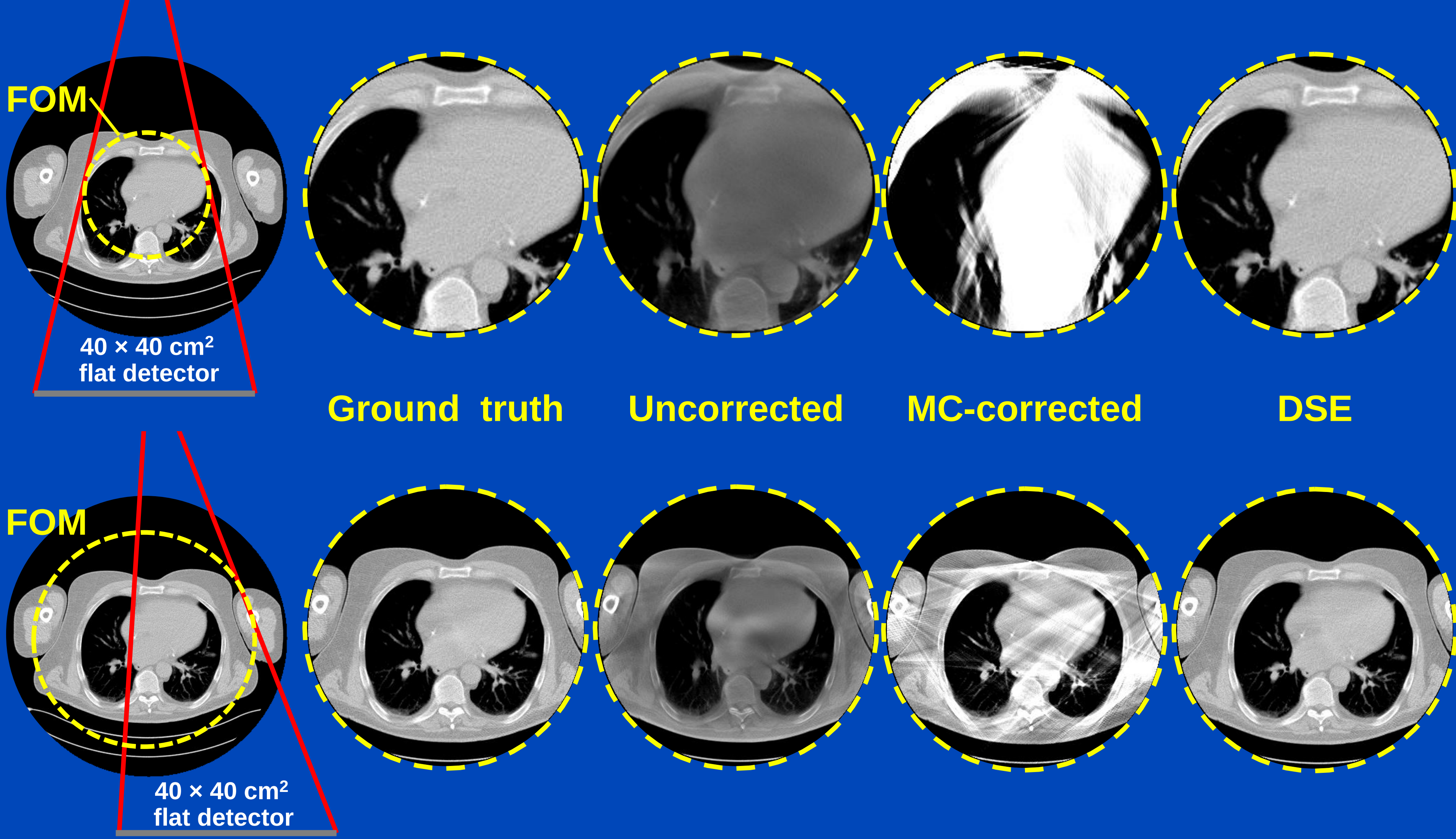

To learn why MC fails at truncated data and what significant efforts are necessary to cope with that situation see [Kachelrieß et al. Effect of detruncation on the accuracy of MC-based scatter estimation in truncated CBCT. Med. Phys. 45(8):3574-3590, August 2018].

J. Maier, M. Kachelrieß et al. Deep scatter estimation (DSE). SPIE 2017 and Journal of Nondestructive Evaluation 37:57, July 2018.
J. Maier, M. Kachelrieß et al. Robustness of DSE. Med. Phys. 46(1):238-249, January 2019.

Scatter in Dual Source CT (DSCT)

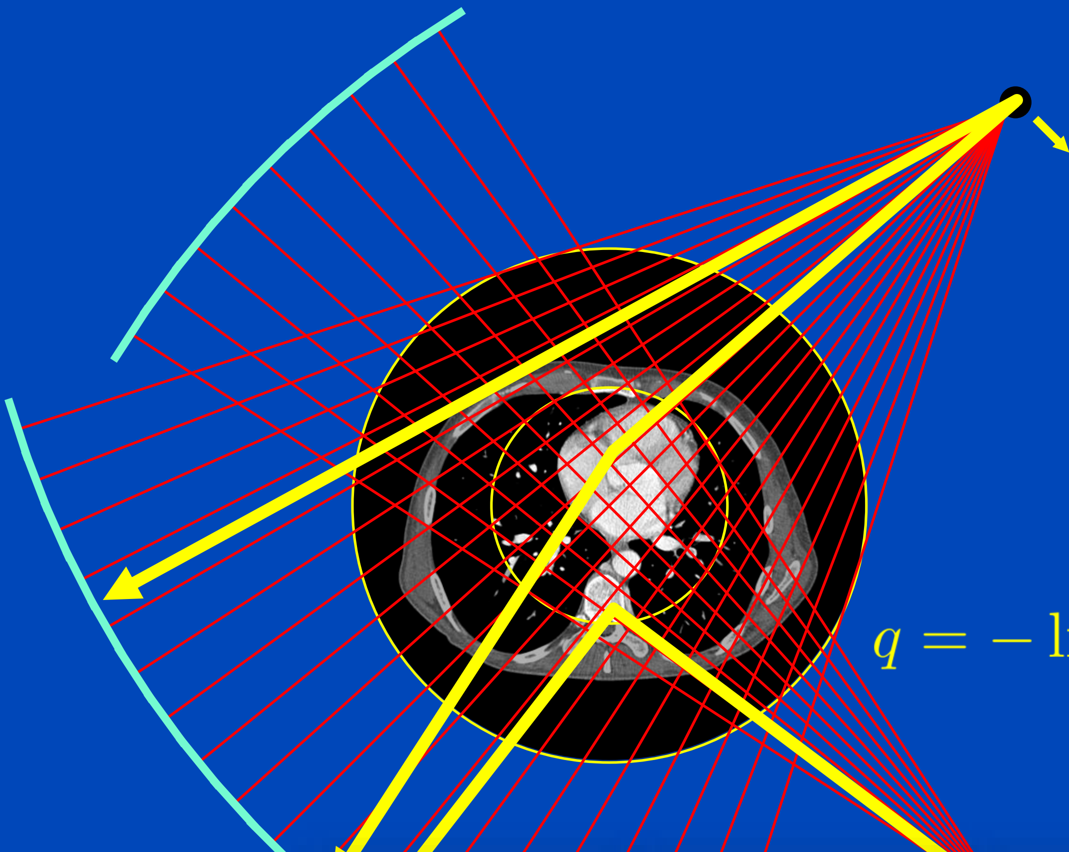

Siemens SOMATOM Force
dual source cone-beam spiral CT

$$q = -\ln \frac{I_{\text{primary}} + S_{\text{forward}} + \rho\, S_{\text{cross}}}{I_0}$$

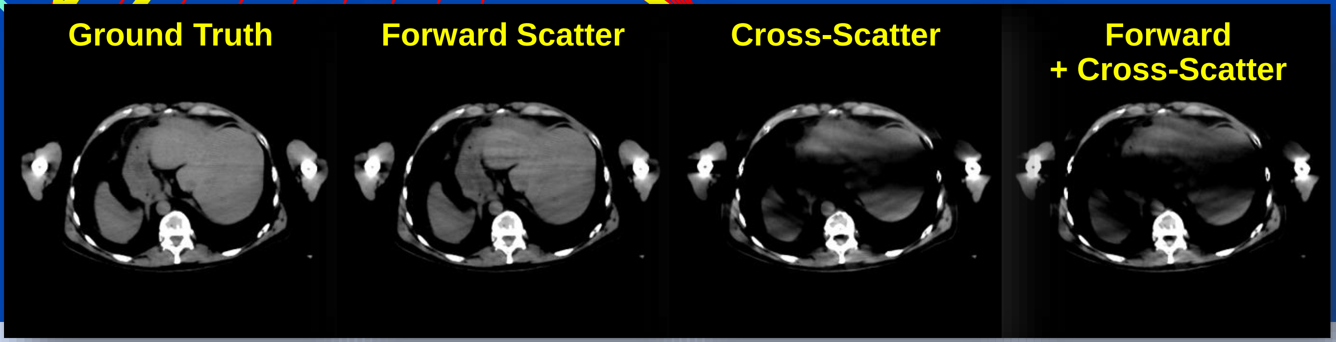

C = 40 HU, *W* = 300 HU, with 2D anti-scatter grid

dkfz.

Scatter in Dual Source CT: xDSE

Ground Truth | **Uncorrected** | **xDSE (2D, xSSE)** | **Measurement-based**

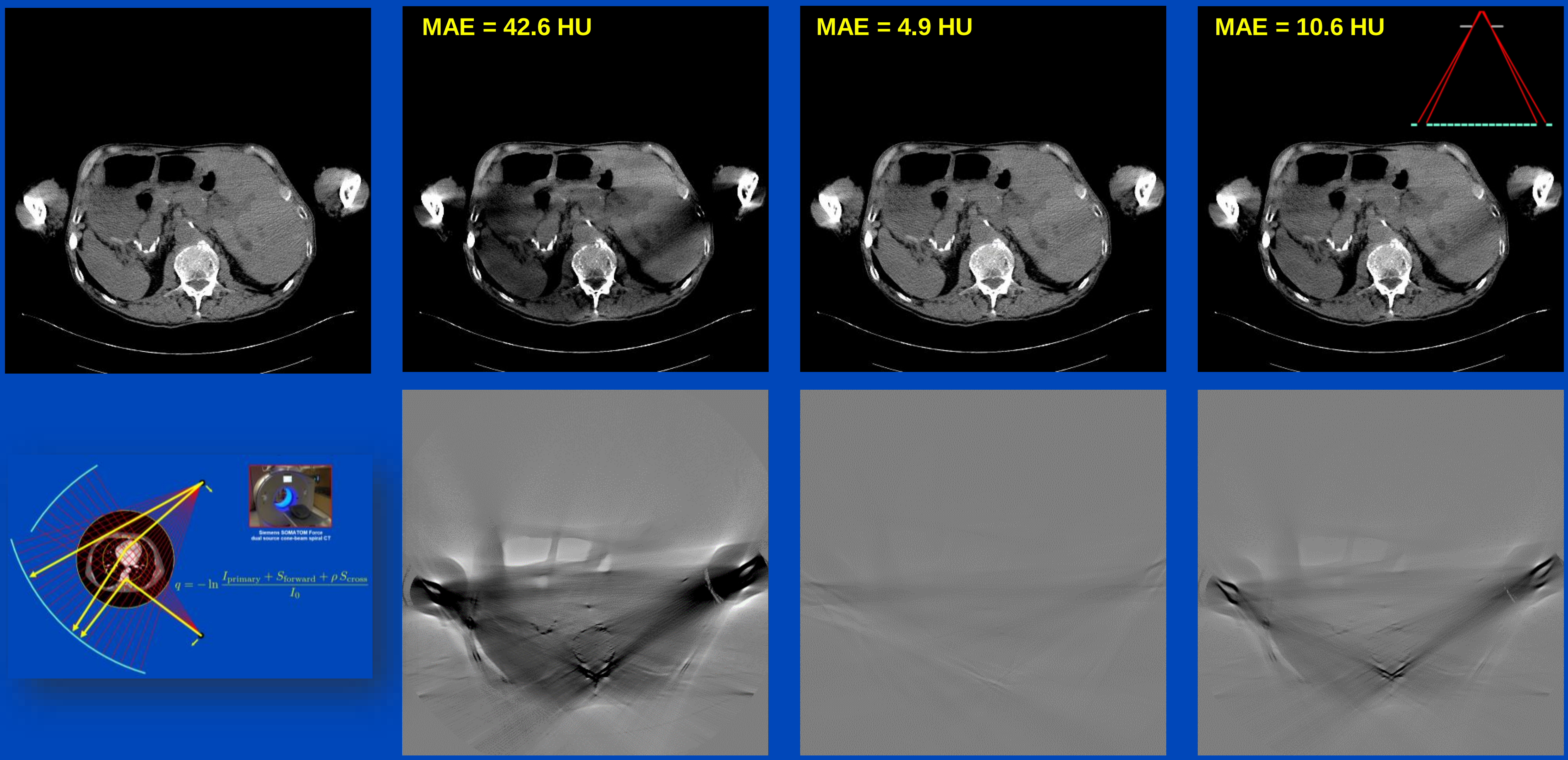

xDSE (2D, xSSE) maps
primary + forward scatter + cross-scatter + cross-scatter approximation → cross-scatter

Images C = 40 HU, W = 300 HU, difference images C = 0 HU, W = 300 HU

J. Erath, M. Kachelrieß et al. Deep learning-based forward and cross-scatter correction in dual source CT. Med. Phys. 48:4824-4842, July 2021.

Scatter for Coarse ASG

Energy-integrating detector

Conventional ASG
Each pixel surrounded by ASG

Photon-counting detector

Coarse ASG
Several pixels surrounded by ASG

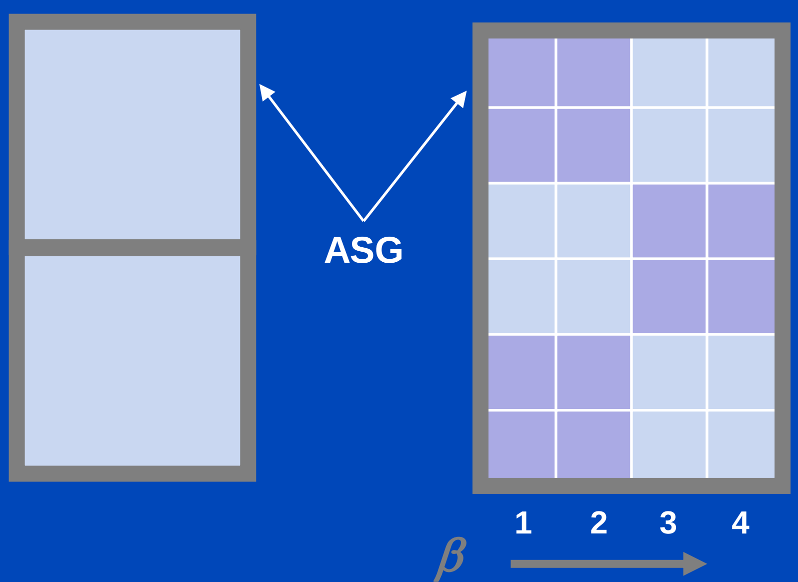

Primary radiation
Scatter measured by the detector
Scatter attenuated by the ASG

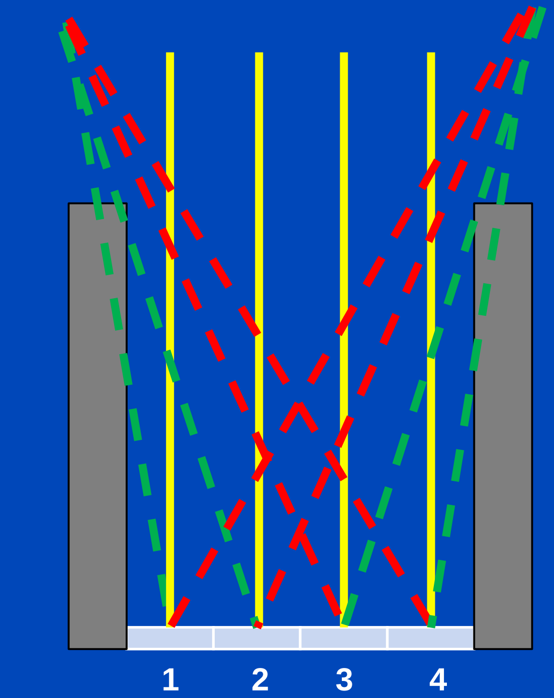

The coarse ASG leads to changes in scatter intensity between neighboring pixels, depending on the incident angle of the photon.

J. Erath, M. Kachelrieß et al. Deep scatter estimation for coarse anti-scatter grids as used in photon-counting CT. Proceedings of the 7th International Conference on Image Formation in X-Ray Computed Tomography:190-193, June 2022.

Scatter for Coarse ASG

Four subpixels (S) merged to one macropixel (M)

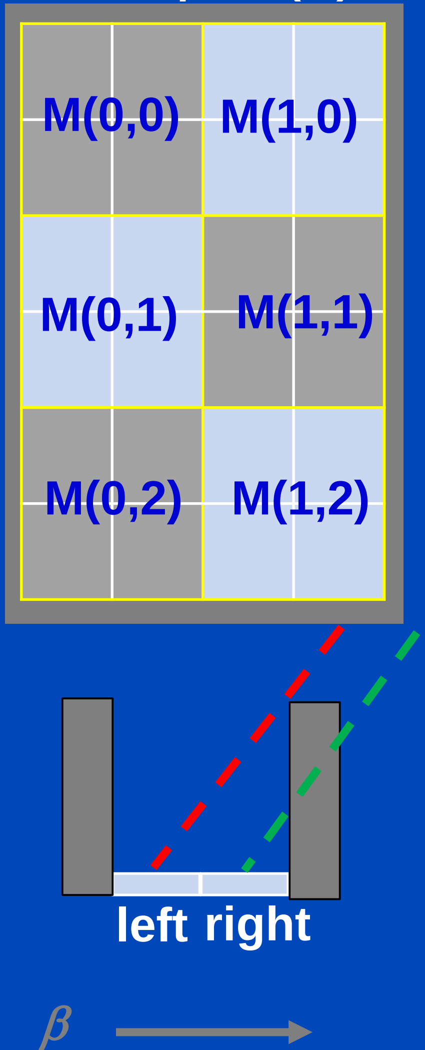

Scatter distribution averaged over all detector rows

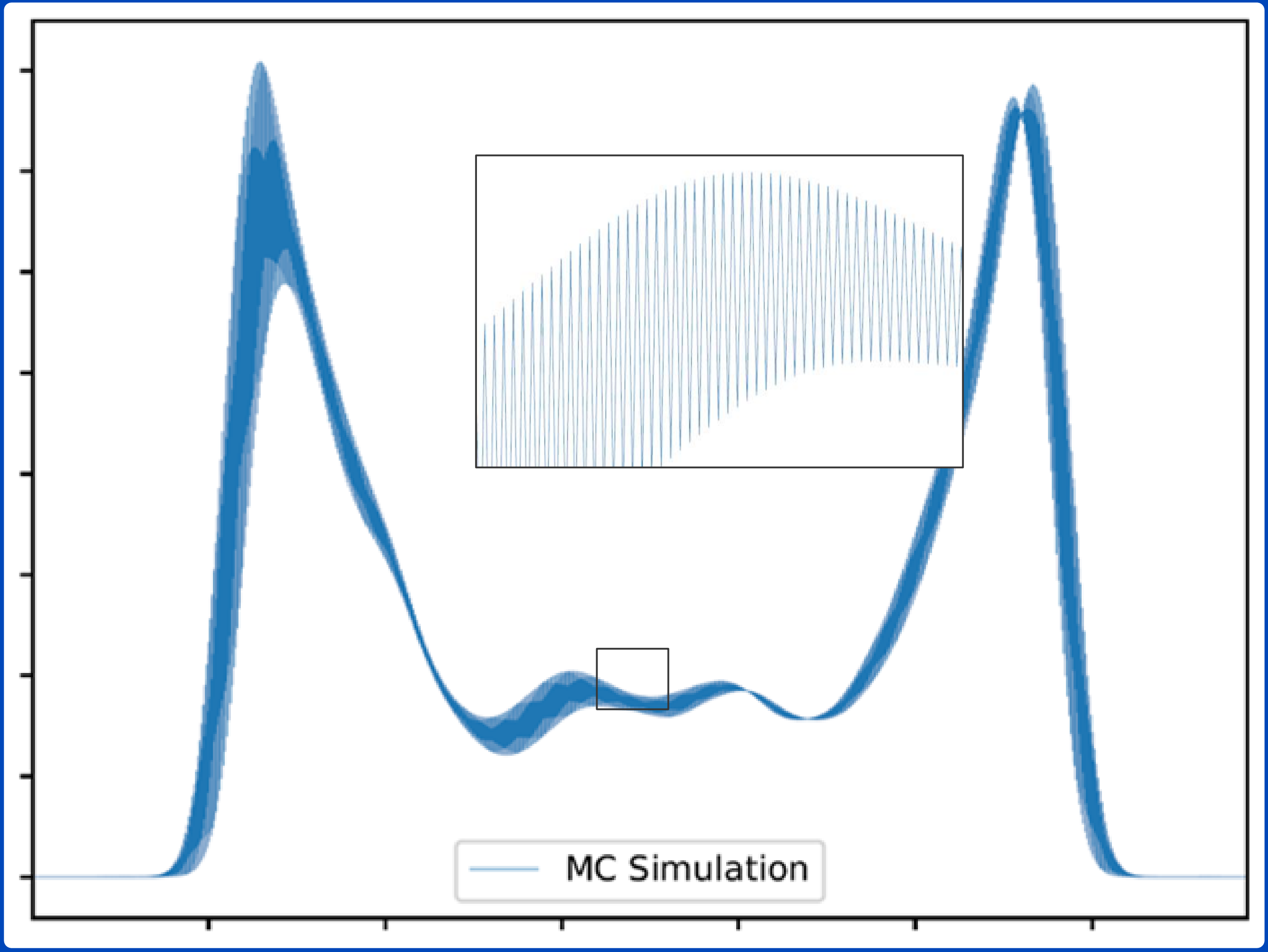

Detector columns

J. Erath, M. Kachelrieß et al. Deep scatter estimation for coarse anti-scatter grids as used in photon-counting CT. Proceedings of the 7th International Conference on Image Formation in X-Ray Computed Tomography:190-193, June 2022.

dkfz.

Scatter for Coarse ASG

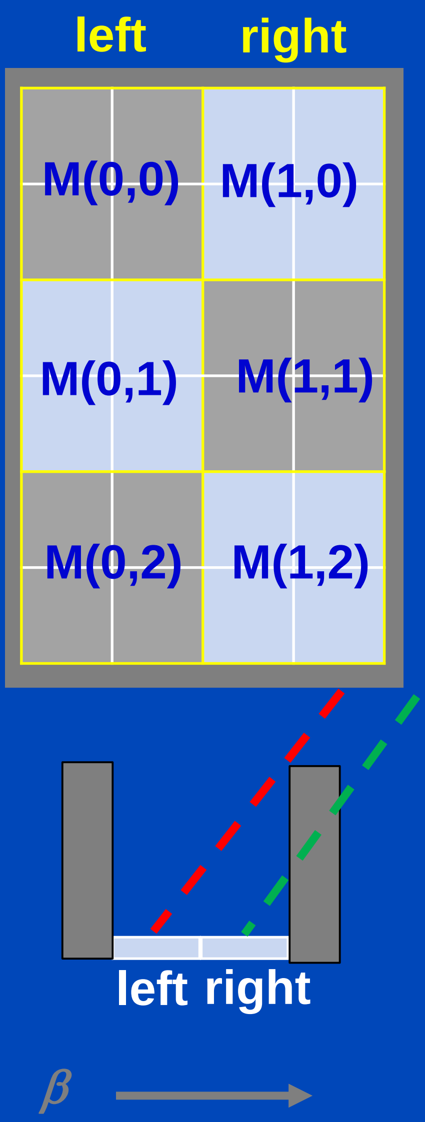

Scatter distribution averaged over all detector rows

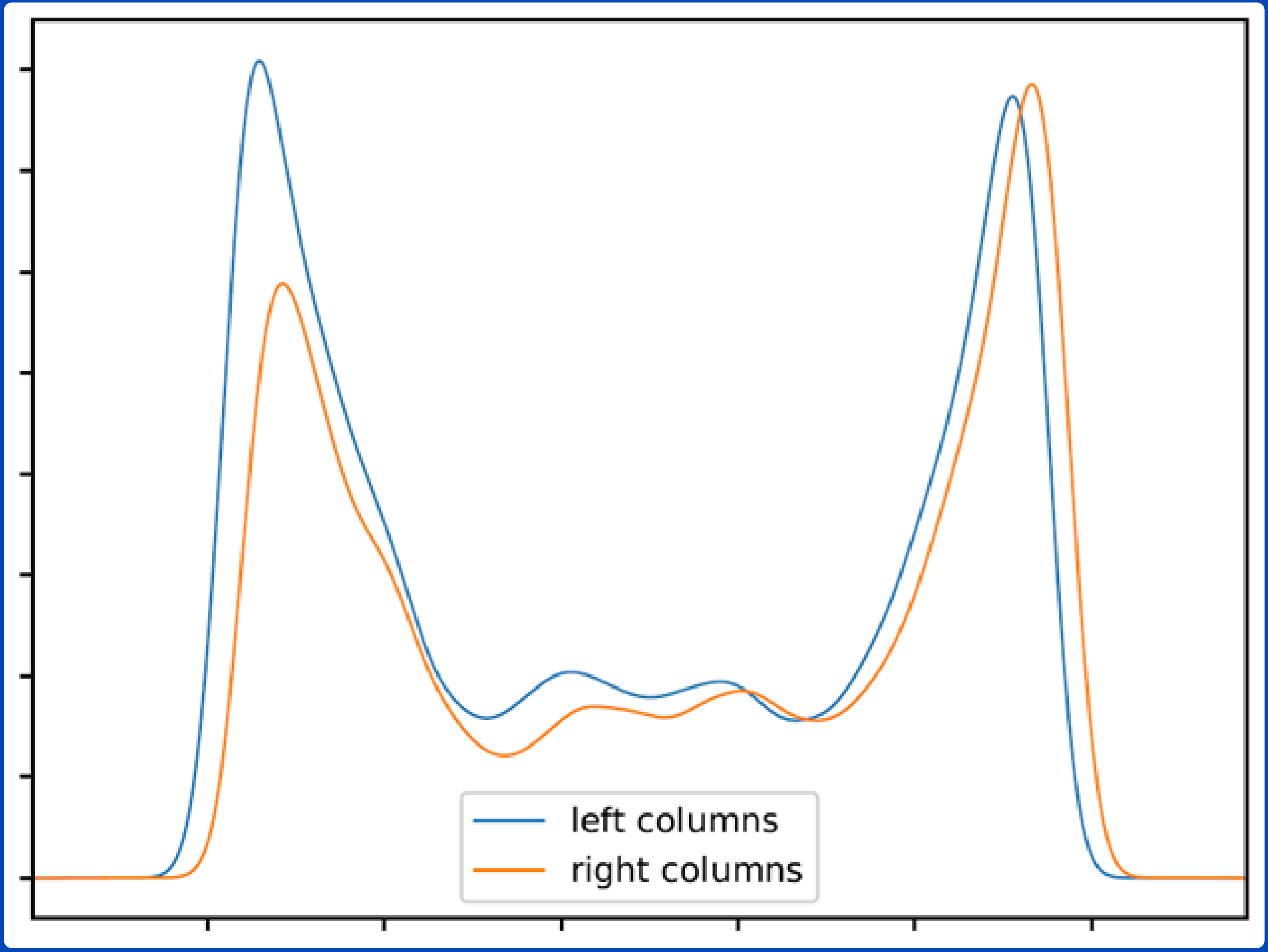

Detector columns

J. Erath, M. Kachelrieß et al. Deep scatter estimation for coarse anti-scatter grids as used in photon-counting CT. Proceedings of the 7th International Conference on Image Formation in X-Ray Computed Tomography:190-193, June 2022.

Scatter Artifacts of Coarse ASG

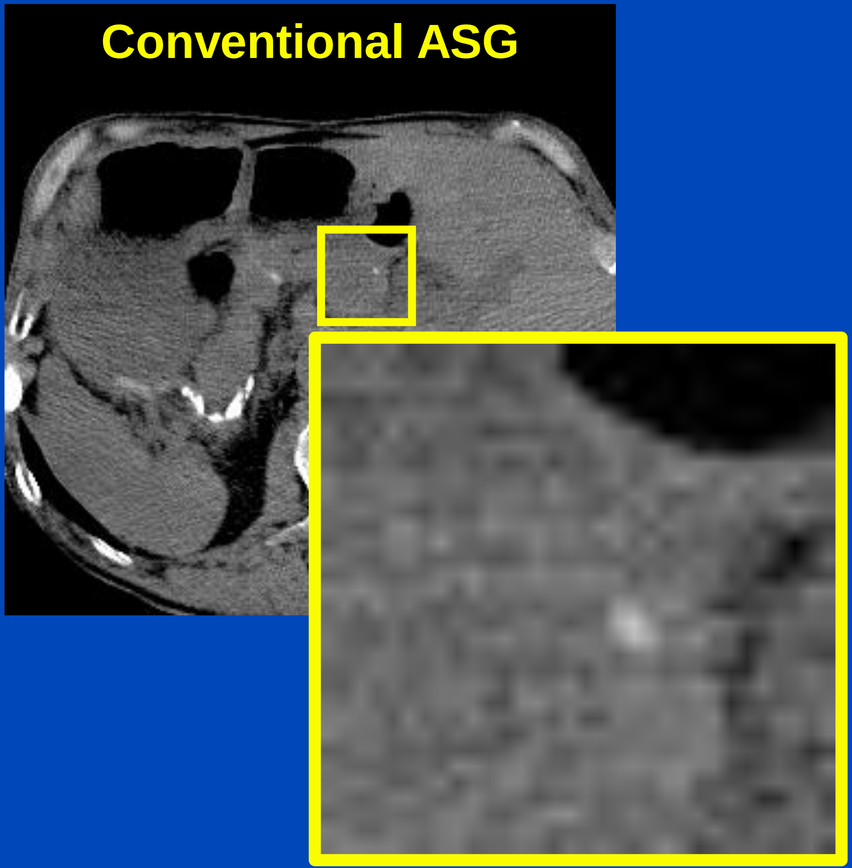

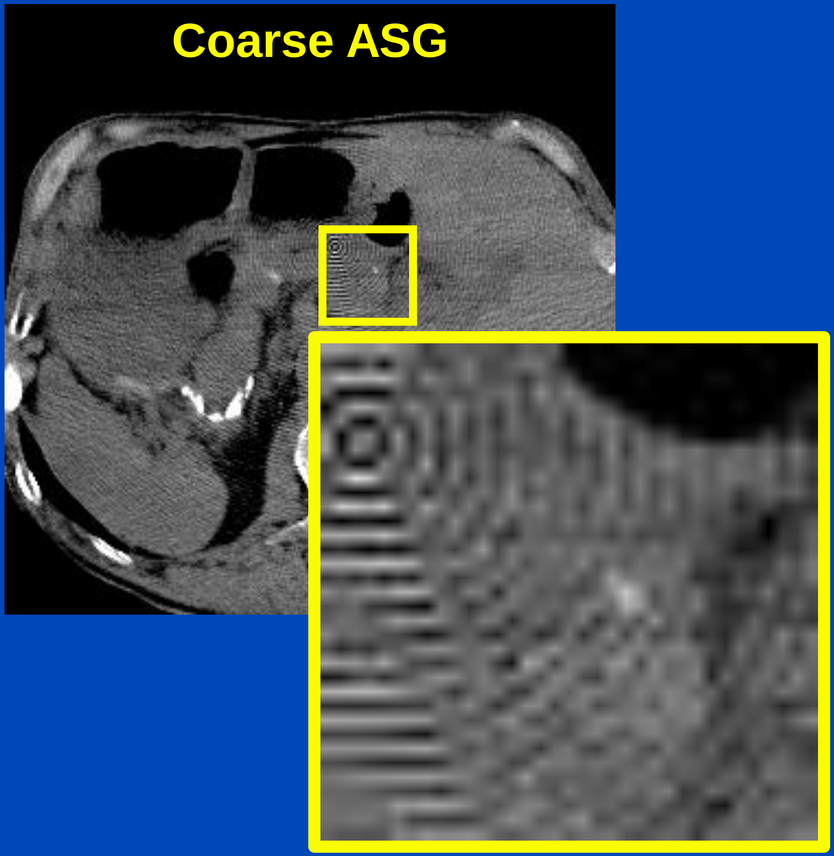

Coarse ASGs can lead to scatter-induced moiré artifacts.

Reconstruction: *C* = 40 HU, *W* = 300 HU

Network Architecture

Detector dimension
1376×144
Input mapping

$$p = -\ln\left(\frac{I_{\text{primary}}}{I_0} + \frac{I_{\text{scatter}}}{I_0}\right)$$

Each channel corresponds to a different pixel position between the lamellae of the ASG

Merging 6 different channels to obtain total scatter correction term

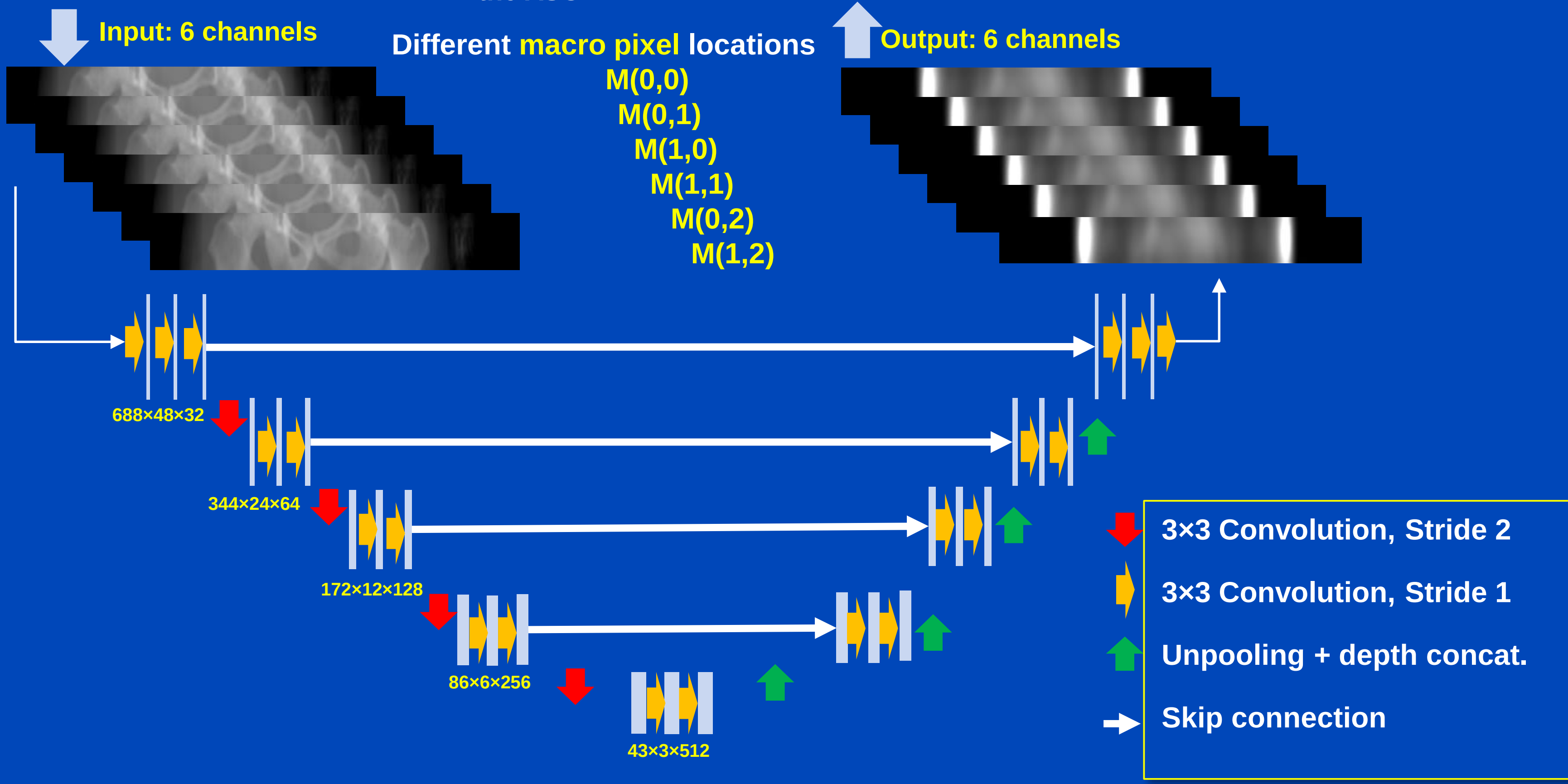

J. Erath, M. Kachelrieß et al. Deep scatter estimation for coarse anti-scatter grids as used in photon-counting CT. Proceedings of the 7th International Conference on Image Formation in X-Ray Computed Tomography:190-193, June 2022.

dkfz.

Results in Reconstructed Images

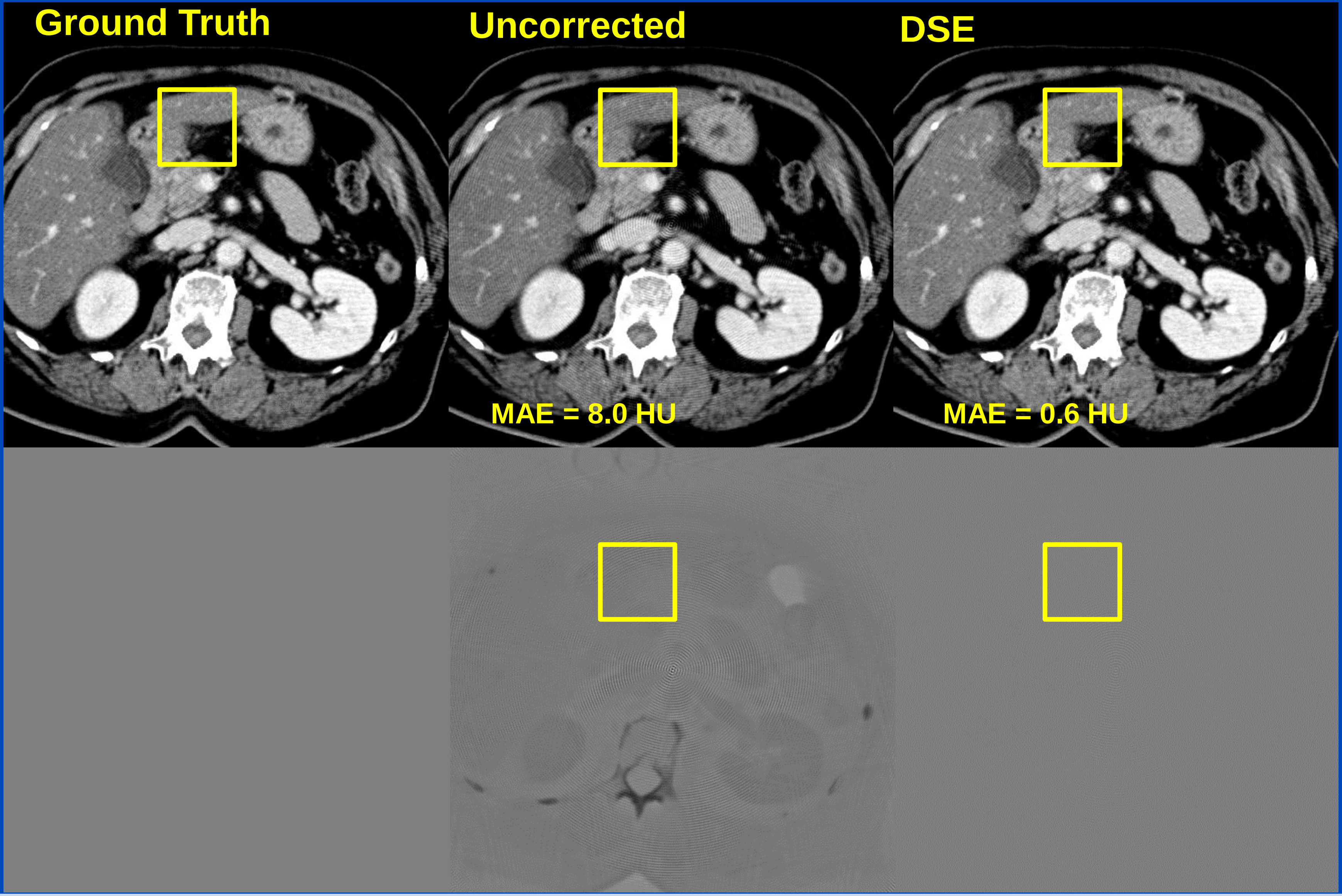

Simulated Reconstruction *C* = 0 HU, *W* = 400 HU,
Difference to GT *C* = 0 HU, *W* = 50 HU

Results in Reconstructed Images

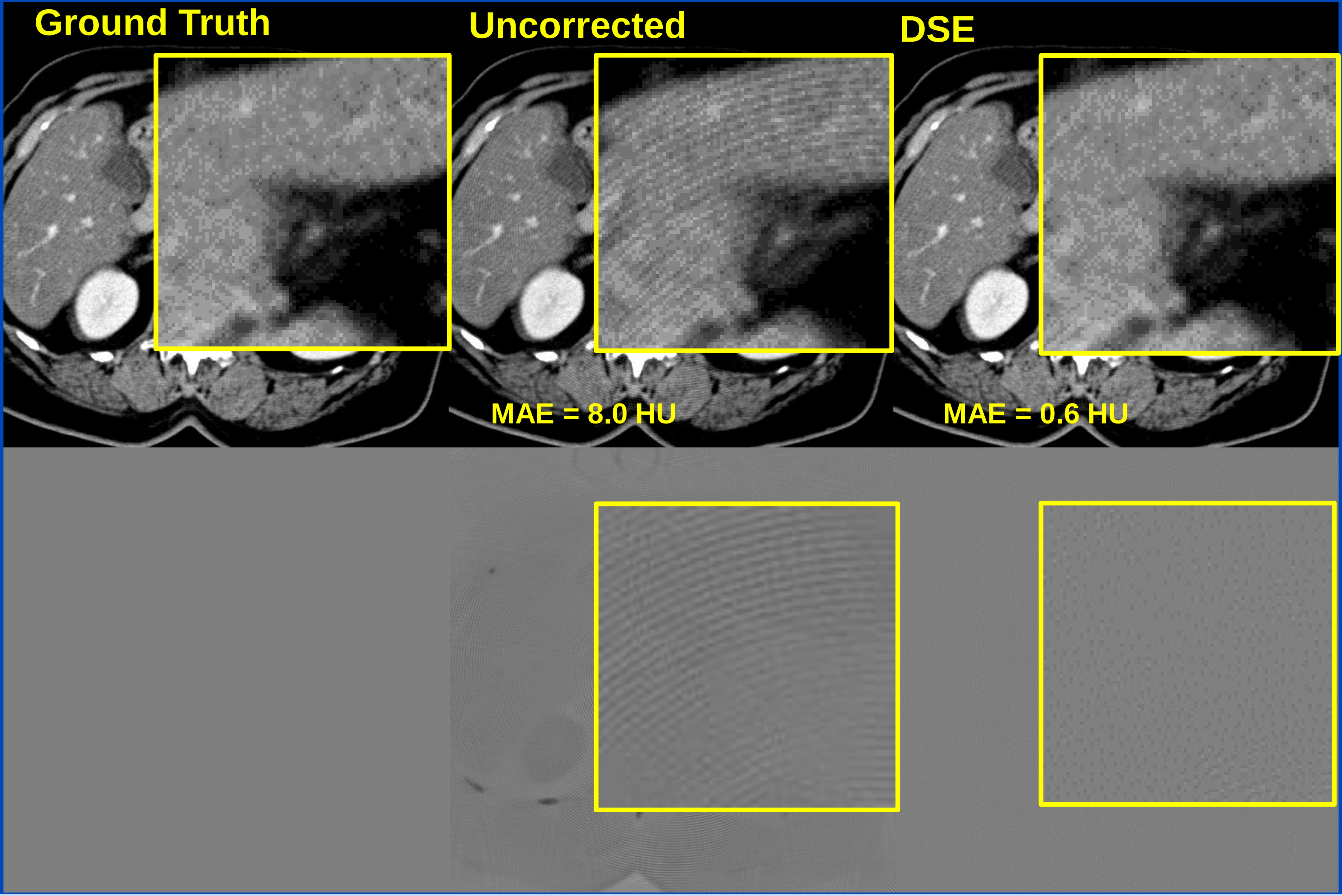

Simulated Reconstruction C = 0 HU, W = 400 HU,
Difference to GT C = 0 HU, W = 50 HU

Conclusions on DSE

- DSE needs about 3 ms per CT projection (as of 2020).
- DSE is a fast and accurate alternative to MC simulations.
- DSE outperforms other approaches.
- Facts:
  - DSE can estimate scatter from a single (!) x-ray image.
  - DSE can accurately estimate scatter from a primary+scatter image.
  - DSE generalizes to all anatomical regions.
  - DSE works for geometries and beam qualities differing from training.
  - DSE may outperform MC even though DSE is trained with MC.
- DSE is not restricted to reproducing MC scatter estimates. It can be trained with any other scatter estimate, including those based on measurements.

Deep Cardiac Motion Compensation

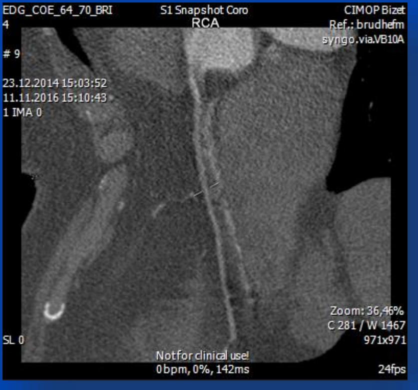

???

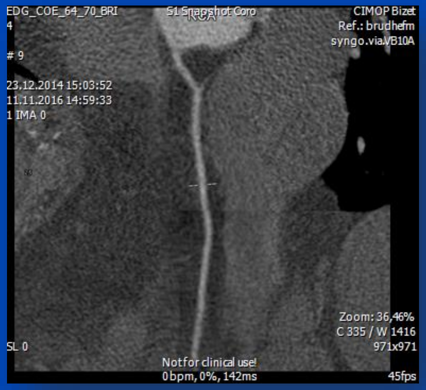

PAMoCo

Generate 2K+1 Partial Angle Reconstructions

Initial segmented stack volume

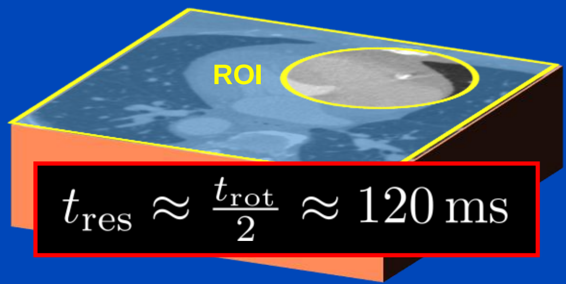

$$t_{\mathrm{res}} \approx \frac{t_{\mathrm{rot}}}{2} \approx 120\,\mathrm{ms}$$

Subdivide the projection data $p'(\vartheta, \xi)$
into 2K + 1 overlapping sectors

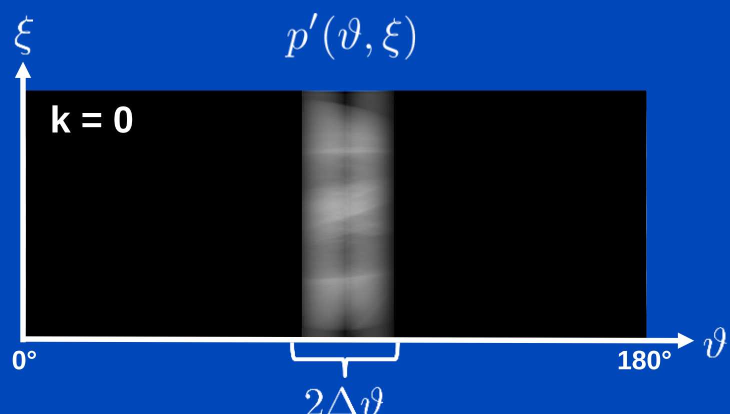

$$p_k(\vartheta, \xi) = w_k(\vartheta) p'(\vartheta, \xi)$$
$$w_k(\vartheta) = \Lambda((\vartheta - \vartheta_k)/2\Delta\vartheta)$$

Partial angle reconstructions $f_k(\boldsymbol{r})$

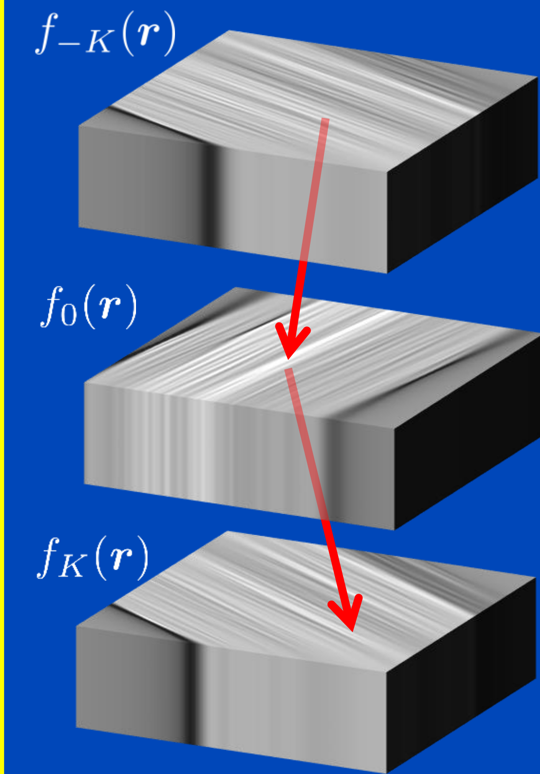

$$t_{\mathrm{res}} \approx \frac{t_{\mathrm{rot}}/2}{(2K+1)/2} \approx 10\,\mathrm{ms}$$

FWHM = $\Delta\vartheta$ **K = 12**

J. Hahn, M. Kachelrieß et al. Motion compensation in the region of the coronary arteries based on partial angle reconstructions from short scan CT data. Med. Phys. 44(11):5795-5813, September 2017.

Deep PAMoCo

Network architecture

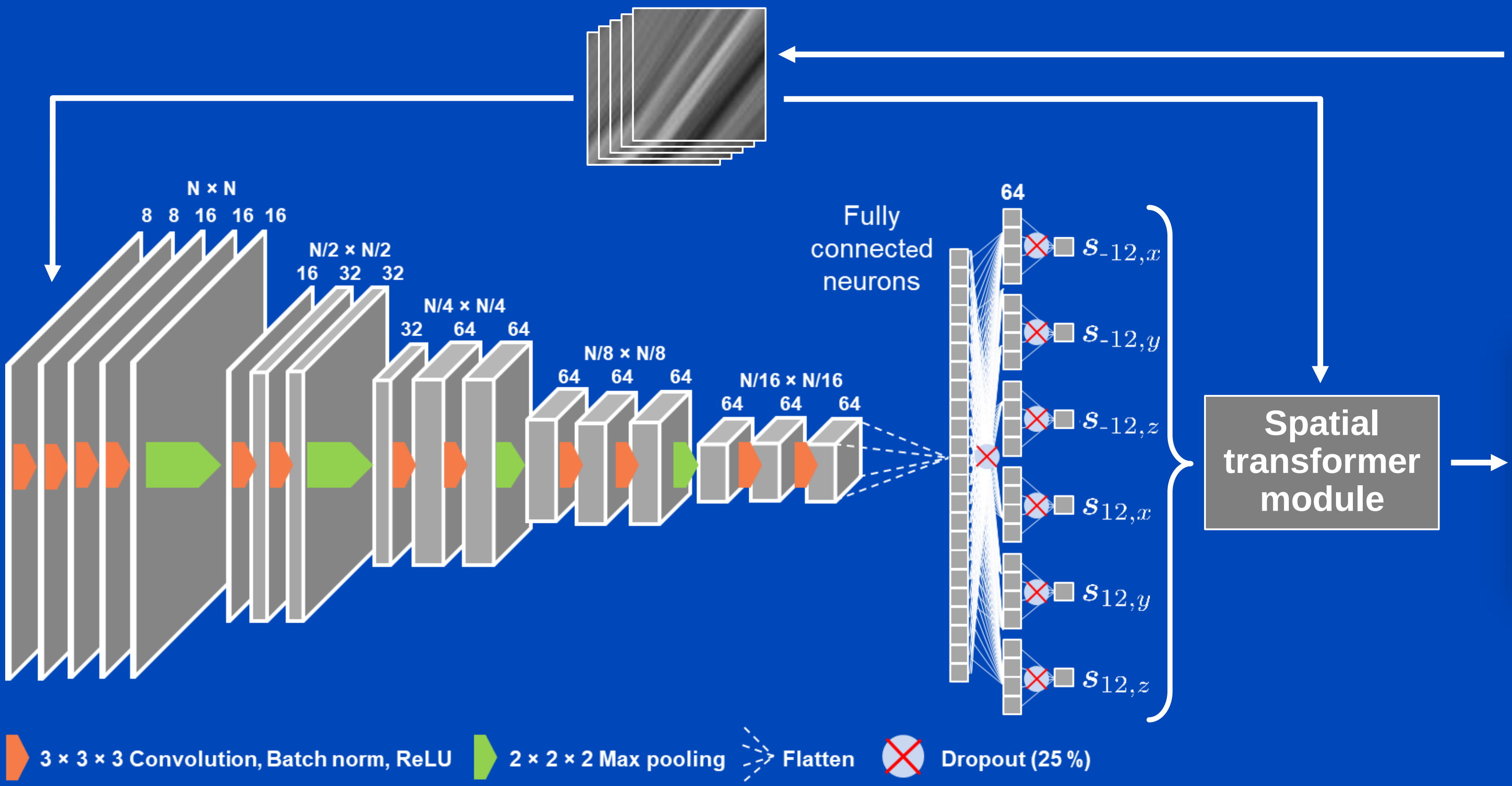

Initial volume

(with motion artifacts)

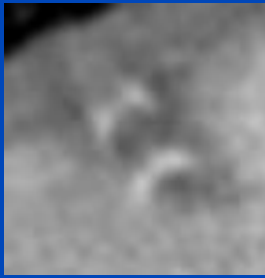

Final volume

(no motion artifacts)

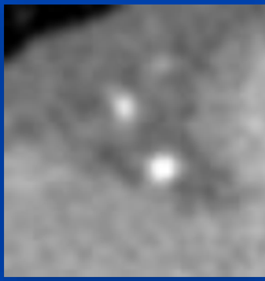

FCN-Layer output: two control points for a cubic spline: for $k = -K$, and for $k = +K$. The third control point at $k = 0$ is (0, 0, 0), i.e. no deformation for the central PAR.

J. Maier, S. Lebedev, J. Erath, E. Eulig, S. Sawall, E. Fournié, K. Stierstorfer, M. Lell, and M. Kachelrieß. Deep learning-based coronary artery motion estimation and compensation for short-scan cardiac CT. Med. Phys. 48(7):3559-3571, July 2021.

Results

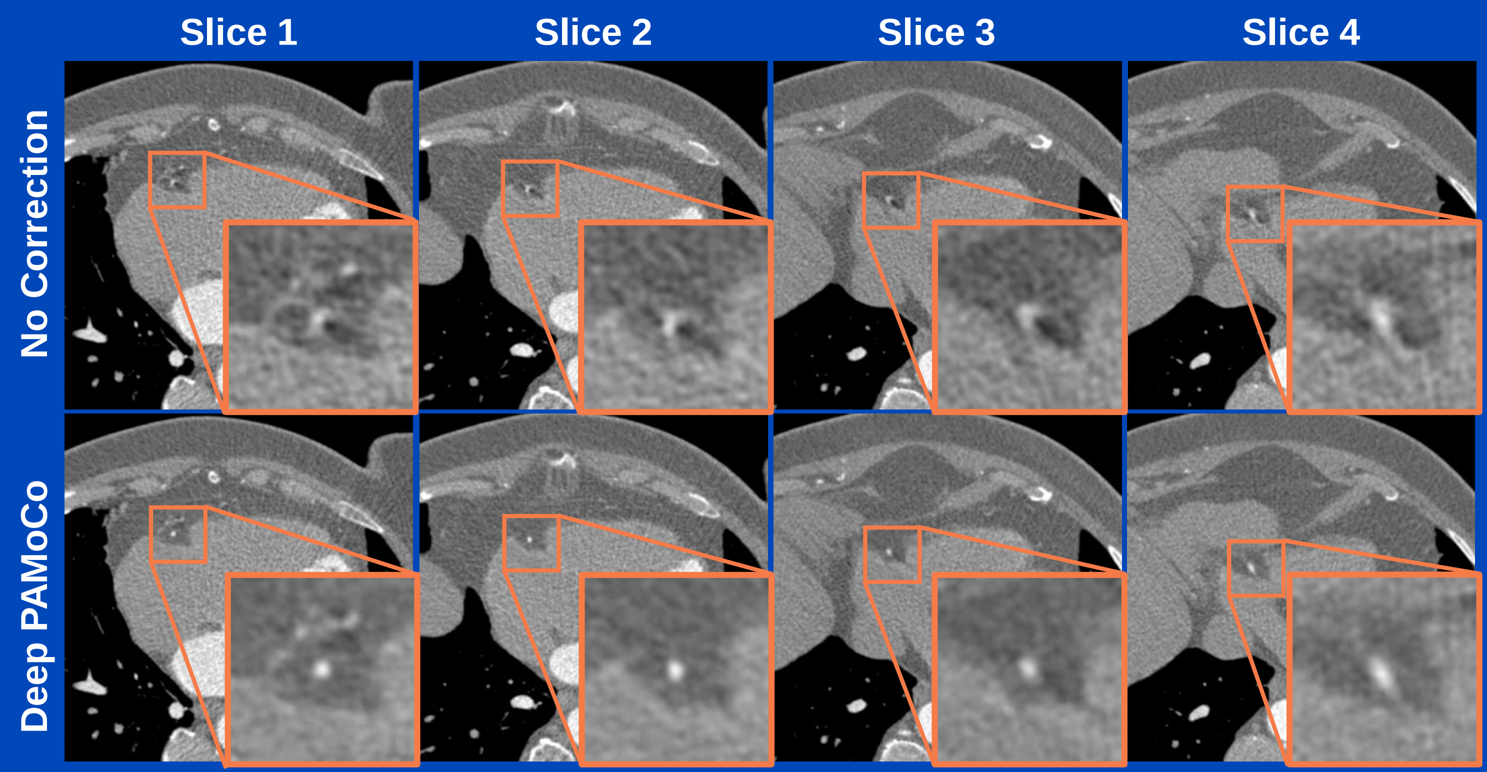

C = 1000 HU
W = 1000 HU

J. Maier, S. Lebedev, J. Erath, E. Eulig, S. Sawall, E. Fournié, K. Stierstorfer, M. Lell, and M. Kachelrieß. Deep learning-based coronary artery motion estimation and compensation for short-scan cardiac CT. Med. Phys. 48(7):3559-3571, July 2021.

Results

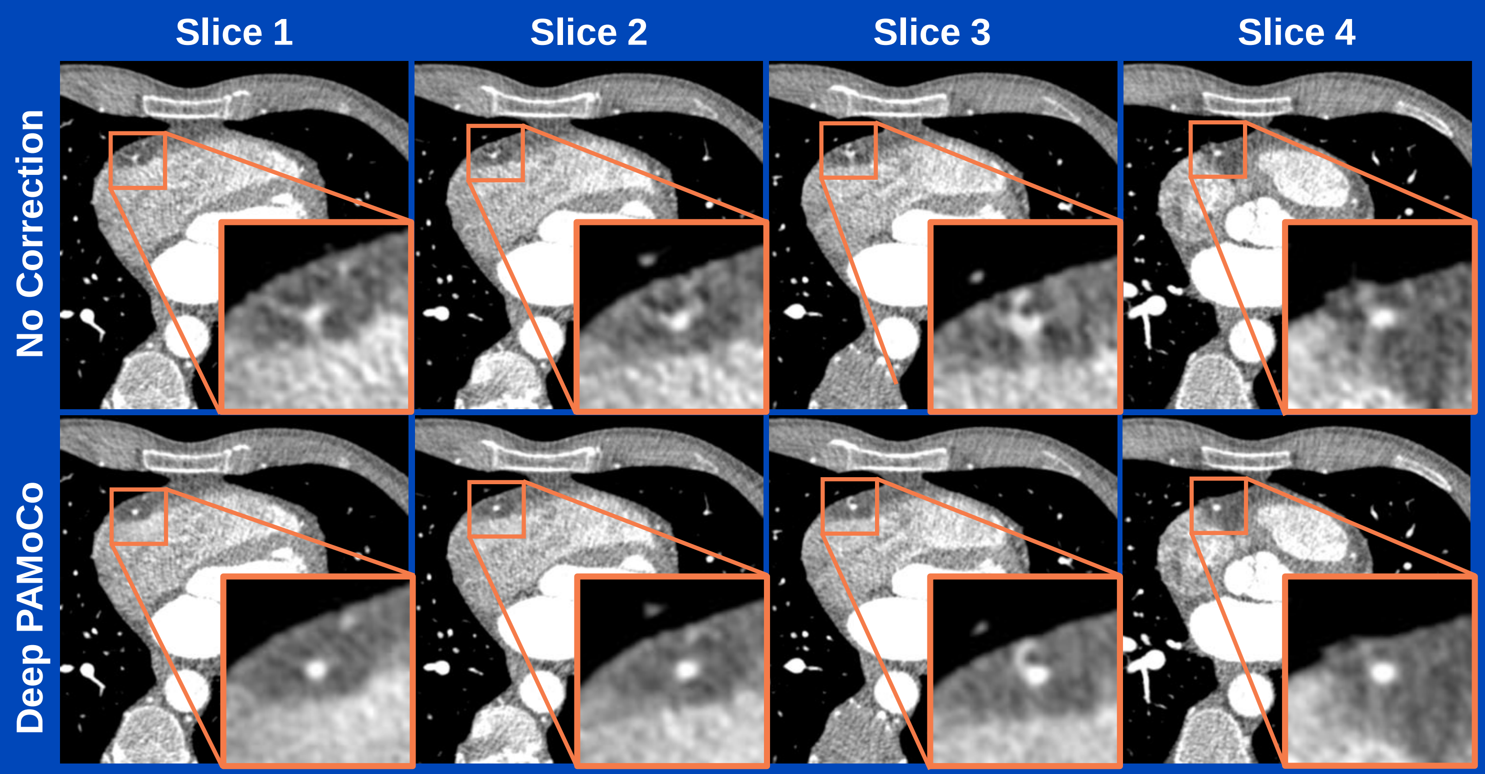

C = 1000 HU
W = 1000 HU

Results

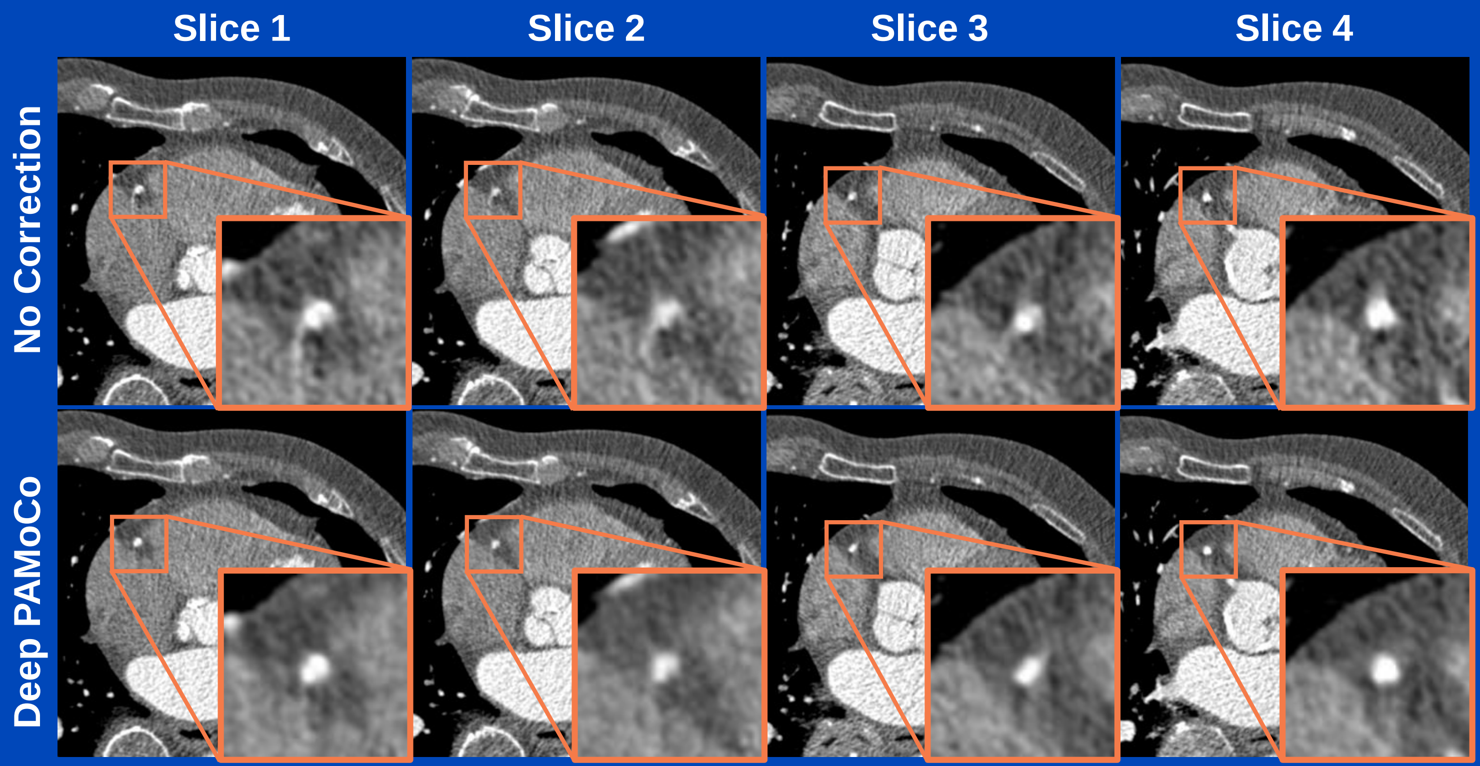

C = 1100 HU
W = 1000 HU

J. Maier, S. Lebedev, J. Erath, E. Eulig, S. Sawall, E. Fournié, K. Stierstorfer, M. Lell, and M. Kachelrieß. Deep learning-based coronary artery motion estimation and compensation for short-scan cardiac CT. Med. Phys. 48(7):3559-3571, July 2021.

Are the Methods Reliable?

- Studies about explainability of AI in CT image formation are more than sparse.
- My thoughts:
  - Cosmetic corrections: Unclear if noise reduction, metal artifact reduction etc. is removing/adding lesions. The whole process is a black box.
  - Physical corrections: A clear physical meaning and rawdata fidelity appear more reliable. Examples:
    - » MAR or detruncation networks where the NN output is used only to forward project and inpaint/extrapolate the rawdata
    - » Scatter correction that estimates a smooth physically realistic (trained with MC) scatter signal in intensity domain
    - » Motion correction networks that estimate motion vectors rather than manipulating the voxel values

Thank You!

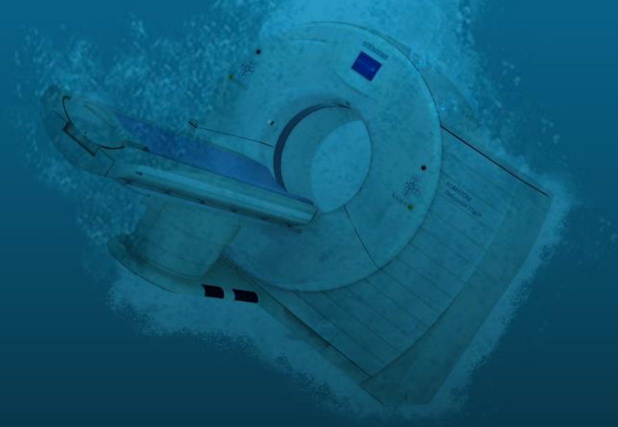

This presentation will soon be available at www.dkfz.de/ct.

Job opportunities through DKFZ’s international PhD or Postdoctoral Fellowship programs (marc.kachelriess@dkfz.de).

Parts of the reconstruction software were provided by RayConStruct® GmbH, Nürnberg, Germany.